UNIVERSIDADE ESTADUAL PAULISTA - UNESP

CÂMPUS DE JABOTICABAL

MODELS FOR ESTIMATION GROWTH, YIELD AND NUTRIENTS CONTENT OF PROCESSING TOMATO

Juliana Aparecida dos Santos da Silva

Engenheira Agrônoma

2016

UNIVERSIDADE ESTADUAL PAULISTA - UNESP

CÂMPUS DE JABOTICABAL

MODELS FOR ESTIMATION GROWTH, YIELD AND NUTRIENTS CONTENT OF PROCESSING TOMATO

Juliana Aparecida dos Santos da Silva

Orientador: Prof. Dr. Arthur Bernardes Cecílio Filho

Coorientador: Prof. Dr. Glauco de Souza Rolim

Tese apresentada à Faculdade de Ciências Agrárias e Veterinárias – Unesp, Câmpus de Jaboticabal, como parte das exigências para a obtenção do título de Doutora em Agronomia (Produção Vegetal)

2016

Silva, Juliana Aparecida dos Santos da
S586m Models for estimation growth, yield and nutrients content of processing tomato / Juliana Aparecida dos Santos da Silva. – – Jaboticabal, 2016
vi, 82 p. : il. ; 29 cm

Tese (doutorado) - Universidade Estadual Paulista, Faculdade de Ciências Agrárias e Veterinárias, 2016
Orientador: Arthur Bernardes Cecílio Filho
Banca examinadora: Renato de Mello Prado, José Ricardo Mantovani, Jairo Osvaldo Cazetta, Adriano Bortolotti da Silva
Bibliografia

1. Horticultura. 2. Modelagem de culturas. 3. Tomate. I. Título. II. Jaboticabal-Faculdade de Ciências Agrárias e Veterinárias.

CDU 631,811:635,64

Ficha catalográfica elaborada pela Seção Técnica de Aquisição e Tratamento da Informação – Serviço Técnico de Biblioteca e Documentação - UNESP, Câmpus de Jaboticabal.

UNIVERSIDADE ESTADUAL PAULISTA

Câmpus de Jaboticabal

CERTIFICADO DE APROVAÇÃO

TÍTULO: MODELS FOR ESTIMATION GROWTH, YIELD AND NUTRIENTS CONTENT OF PROCESSING TOMATO

AUTORA: JULIANA APARECIDA DOS SANTOS DA SILVA
ORIENTADOR: ARTHUR BERNARDES CECILIO FILHO
COORIENTADOR: GLAUCO DE SOUZA ROLIM

Aprovada como parte das exigências para obtenção do Título de Doutora em AGRONOMIA (PRODUÇÃO VEGETAL), pela Comissão Examinadora:

Prof. Dr. ARTHUR BERNARDES CECILIO FILHO
Departamento de Produção Vegetal / FCAV / UNESP - Jaboticabal

Prof. Dr. RENATO DE MELLO PRADO
Departamento de Solos e Adubos / FCAV / UNESP - Jaboticabal

Prof. Dr. JOSÉ RICARDO MANTOVANI
Instituto de Ciências Agrárias / UNIFENAS - Alfenas/MG

Prof. Dr. JAIRO OSVALDO CAZETTA
Departamento de Tecnologia / FCAV / UNESP - Jaboticabal

Prof. Dr. ADRIANO BORTOLOTTI DA SILVA
Instituto de Ciências Agrárias / UNIFENAS - Alfenas,MG

Jaboticabal, 04 de novembro de 2016.

DADOS CURRICULARES DA AUTORA

JULIANA APARECIDA DOS SANTOS DA SILVA – Nasceu em 24 de junho de 1985, na cidade de São Lourenço – MG. Concluiu o curso de graduação em Engenharia Agronômica pela Universidade José do Rosário Vellano (UNIFENAS), na cidade de Alfenas – MG em dezembro de 2009, onde além das atividades curriculares desenvolveu trabalhos como estagiária e bolsista de iniciação científica (PIBIC) pelo CNPq no laboratório de Biotecnologia Vegetal. Em agosto de 2010, iniciou o curso de Mestrado em Agronomia (Produção Vegetal) na Faculdade de Ciências Agrárias e Veterinárias (FCAV/UNESP) de Jaboticabal – SP, com bolsa concedida pelo Conselho Nacional de Desenvolvimento Científico e Tecnológico - CNPq (processo 153437/2010-3) e conclusão em novembro de 2012. Em março de 2013, iniciou o curso de Doutorado em Agronomia (Produção Vegetal) na Faculdade de Ciências Agrárias e Veterinárias (FCAV/UNESP) de Jaboticabal – SP, com bolsa da Capes (Comissão de Aperfeiçoamento de Pessoal do Nível Superior). Realizou doutorado sanduíche pelo programa PSDE-Capes (processo 000658/2015-04) na Universidade da Flórida em Gainesville - FL no período de 01/05/2015 à 31/01/2016. Concluiu o doutorado em novembro de 2016.

DEDICATÓRIA

Aos meus pais Aristeu e Maria Lúcia, pelo amor e confiança sempre depositados e por estarem sempre presentes nas horas difíceis.

À minha irmã Ana e meus sobrinhos: Bárbara, Nina e Samuel, pois a família é a maior riqueza e alegria que podemos ter.

Ao meu namorado Aluísio, pelo companheirismo e pela força dada todos os dias.

Dedico

AGRADECIMENTOS

À Deus por me dar força e me manter perseverante para concluir o doutorado.

À Faculdade de Ciências Agrárias e Veterinárias de Jaboticabal (FCAV/UNESP) pela infraestrutura, aos professores do curso de pós-graduação pelo aperfeiçoamento profissional e ao Programa de Agronomia (Produção Vegetal) pela bolsa de estudos.

À Predilecta Alimentos, pelos auxílios e por ceder as áreas onde foram instalados os experimentos.

Aos Profs. Drs. Arthur Bernardes Cecílio, Glauco de Souza Rolim e Kenneth J. Boote pela orientação, confiança, amizade.

Aos membros da banca examinadora do Exame Geral de Qualificação: Dr. Rogério Teixeira de Faria, Dra. Priscila L. Gratão e Dra Mara Cristina Pessôa da Cruz; e da banca de Defesa: Dr. José Ricardo Mantovani, Dr. Adriano Bortolotti da Silva, Dr. Jairo Osvaldo Cazetta e Dr. Renato de Mello Prado, pela participação e contribuição no enriquecimento deste trabalho.

Aos funcionários da horta didática e da estação agroclimatológica, em especial ao Carlos Alberto, pela atenção, colaboração e ajuda sempre que requisitada.

"A todos aqueles que contribuíram de alguma maneira para o desenvolvimento e realização deste trabalho"

MEUS SINCEROS AGRADECIMENTOS

SUMMARY **Page**

MODELS FOR ESTIMATION GROWTH, YIELD AND NUTRIENTS CONTENT OF PROCESSING TOMATO

ABSTRACT - In this work were discussed processes related to development and growth of processing tomato. The experiments were conducted in the years 2013 and 2014 in three different areas in the city of Guaíra-SP. In chapter 1 the objective was to calibrate and test the CROPGRO-Tomato model with data of five field experiments with processing tomato under different phosphorus concentrations in the soil. The treatments of experiments for calibration were for the area 1: 0, 150, 300, 450, 600 and 750 kg ha^{-1} P_2O_5 and for the areas two and three: 0, 200, 400, 600, 800 and 1000 kg ha^{-1} P_2O_5, in randomized block design with four replications. The experiments for testing the model 450 kg ha^{-1} P_2O_5 was applied. In each 15 days after transplanting (DAT) plants were collected for measuring biomass and leaf area. At the end of crop cycle plants were collected for evaluation of production. All data collected were used for calibration and testing of CROPGRO-Tomato model. The model was accurate (average *d* index = 0.91, average RRMSE = 0.24) to simulate response of processing tomato to different soil P concentrations. The objective of Experiment 2 was to estimate the leaf area index (LAI) of processing tomato using data obtained by destructive and non-destructive methods, meteorological data and number of leaves (NL). For Experiment 2 the methods of measuring leaf area were Li-Cor (destructive), ImageJ and Canopeo (digital images). Also for estimation of LAI it were used sum of degree-days (ΣDD), global radiation (Qg) and number of leaves (NL). Photographs were taken at random, in two different areas at 15, 30, 45, 60, 75, 90, 105, DAT 120 using a $1m^2$ square frame placed over the plants. Photographs were taken in 24 different points, in each point it was collected one plant for leaf area measurement using Li-Cor and leaves counting. LAI estimation using Canopeo and NL were the most accurated with RMSE=0.4, *es*= 0.7, R^2= 0.93 and RMSE = 0.2, *se* = 0.7 and R^2 = 0.92, respectively. It is possible to estimate LAI of processing tomato using non-destructive and low cost methods. The objective of Experiment 3 was to characterize the accumulation of biomass and nutrients in processing tomatoes grown in high and low fertility soils. Plants were collected in four replications (3 plants per replication), every ten days (30 to 120 DAT). After cleaned and dried the material was used to determine nutrient content and biomass. Data were adjusted to

polynomial regressions. The decreasing order of nutrient accumulation was K, N, Ca, P, Mg, S, Fe, Cu, Mn, Zn in HF; and K, N, Ca, P, Mg, S, Fe, Mn, Cu, Zn in LF. Tomato plants grown in HF and LF soils, however fertilized in the same manner, have similar potential of biomass producing.

Keywords - Crop modeling, plant nutrition, biomass, leaf area

MODELOS PARA ESTIMAR CRESCIMENTO, PRODUTIVIDADE E TEORES DE NUTRIENTES DO TOMATE INDUSTRIAL

RESUMO - Neste trabalho foram estudados processos relacionados ao desenvolvimento e crescimento do tomate industrial. Os experimentos foram conduzidos nos anos 2013 e 2014 em três áreas diferentes da cidade de Guaíra-SP. No capítulo 1, objetivou-se calibrar e testar o modelo CROPGRO-Tomate com dados de cinco experimentos de campo com tomate industrial sob diferentes concentrações de fósforo no solo. Os tratamentos dos experimentos para calibração foram para a área 1: 0, 150, 300, 450, 600 e 750 kg ha^{-1} P_2O_5 e para as áreas dois e três: 0, 200, 400, 600, 800 e 1000 kg ha^{-1} P_2O_5, em delineamento de blocos ao acaso com quatro repetições. Nos experimentos para testar o modelo foi aplicado 450 kg ha^{-1} P_2O_5. A cada 15 dias após o transplante (DAT) plantas foram recolhidas para a medição de biomassa e área foliar. No final do ciclo de cultivo foram coletadas plantas para avaliação da produção. Todos os dados coletados foram utilizados para calibração e teste do modelo CROPGRO-Tomate. O modelo foi acurado (índice *d* médio = 0,91 e RRMSE médio = 0,24) para simular a resposta do tomate industrial à diferentes concentrações de P no solo. O objetivo do experimento 2 foi estimar o índice de área foliar (LAI) do tomate industrial utilizando dados obtidos por métodos destrutivos e não destrutivos, dados meteorológicos e número de folhas (NL). Os métodos de medição da área foliar foram Li-Cor (destrutivo), ImageJ e Canopeo (imagens digitais). Também para a estimativa de LAI foram utilizadas soma de grau-dias (ΣDD), radiação global (Qg) e número de folhas (NL). As fotografias foram tiradas aleatoriamente, em duas áreas diferentes a 15, 30, 45, 60, 75, 90, 105 e120 DAT utilizando um quadro vazado de 1 m^2 de área colocado sobre as plantas. As fotografias foram tiradas em 24 pontos diferentes, em cada ponto foi coletada uma planta para medição da área foliar usando Li-Cor e contagem de folhas. As estimativas LAI usando Canopeo e NL foram mais acuradas com RMSE = 0,4, *se* = 0,7 e R^2 = 0,93; e RMSE = 0,2, *se* = 0,7 e R^2 = 0,92, respectivamente. É possível estimar o IAF de processamento de tomate usando métodos não destrutivos e de baixo custo. O objetivo do experimento 3 foi caracterizar a acumulação de biomassa e nutrientes pelo tomate industrial cultivado em solos de alta (HF) e baixa fertilidade (LF). As plantas foram coletadas em quatro

repetições (3 plantas por replicação) a cada dez dias (30 a 120 DAT). Depois de limpo e seco, o material foi utilizado para determinar o teor de nutrientes e a biomassa. Os dados foram ajustados a regressões polinomiais. A ordem decrescente de acúmulo de nutrientes foi K, N, Ca, P, Mg, S, Fe, Cu, Mn e Zn em HF; e K, N, Ca, P, Mg, S, Fe, Mn, Cu e Zn em LF. As plantas de tomate cultivadas em solos HF e LF, porém fertilizadas da mesma maneira, têm potencial similar de produção de biomassa.

Palavras-chave - Modelagem de culturas, nutrição de plantas, biomassa, área foliar

CHAPTER 1 - GENERAL CONSIDERATIONS

Introduction

Tomato (*Solanum lycopersicum*) is one of vegetable with higher consumption and higher economical importance in the world. It is the second most produced vegetable in the world (FAOSTAT, 2013), and also has the highest area under cultivation among all vegetables (Nangare et al., 2016). The consumption of tomato, either fresh or processed, has increased continuously in the last two decades (Lahoz et al., 2016).

Brazil is among the ten largest producers of tomato in the world, with production up to 4 million tons, this statistic shows the economic importance of this vegetable for the country (FAOSTAT, 2013). In this scenario, the production of processing tomato has increased significantly in recent years. According to estimative by the World Processing Tomato Council - WPTC, Brazilian production of processing tomato is expected to reach 1.35 million tons in 2016, keeping the country in the seventh position of the largest producers (WPTC, 2016).

Due the economical importance of this crop, mathematical models are often used to simulate development and growth of tomato in different environments or managements in order to support decisions and improve production. The advantage in using mathematical models in agronomy is the possibility of simulating the responses of crops to different environmental conditions using determined database, with low cost in reduced time (Naab et al., 2015).

The objective of this study was to use mathematical models, in different approaches to estimate and evaluate the aspects related to development and growth of processing tomato in order to improve understanding of factors related to production such as plant nutrition, soil fertility, leaf area, and accumulation of biomass and nutrients by plants.

Literature review

Processing tomato

The tomato has Andean origin and was introduced in Brazil in the late nineteenth century by European immigrants. It is a perennial shrub, but is grown annually and has two distinct growth habits that influence crop management: indeterminate growth, in which the main stem has apical dominance and grows more than the side stems; determined growth: does not have apical dominance and each stem has a floral branch delimiting its growth (Alvarenga, 2004).

Brazil is the eighth largest producer of tomato in the world (FAOSTAT, 2013). In this scenario, the processing tomato production is highly relevant. According to estimates by the World Processing Tomato Council - WPTC, Brazilian production of processing tomatoes is expected to reach 1.35 million tons in 2016, amount 4% over 2015. The amount produced will keep the country as the seventh largest producer in the world, behind US, China, Italy, Spain, Turkey and Iran (WPTC, 2016).

The area planted with processing tomato in Brazil is about 17,600 hectares and this crop is grown mainly in the Midwest and Southeast. The main producing states are Goiás, São Paulo and Minas Gerais, which account for 69%, 17%, 13% of national production, respectively (Sant'Ana; Nascimento, 2014).

Most of regions in Brazil where the cultivation of processing tomato is larger the soil is acid and have high fixing capacity of phosphorus, therefore this nutrient provides most significant responses in terms of tomato yield increase (Silva; Maluf, 2012).

To achieve high yields tomato plants demand a large amount of nutrients that must be adequately provided due to low natural reserve of Brazilian soil (Silva et al., 2012). Therefore, it is important to know the nutritional requirements in addition to the correct diagnosis of possible soil fertility and plant nutrition problems for the success of culture and the efficient use of fertilizers (Silva et al., 2003).

Despite of the large demand of the culture, nutrient absorption by tomato plants is low in the first 30 days after transplanting (DAT) (Silva et al., 2012; Silva et

al., 2003). With the beginning of flowering and appearance of the first fruits, absorption increases and reaches its maximum in the fruit growth phase, then returns to decline during the ripening of fruits (Silva et al., 2003). Although the pattern of absorption of nutrients by tomato may induce the application of low doses of fertilizers in the initiation of culture, this is not recommended because of the importance of nutrients, for initial development (Silva et al., 2012).

Other important factor that determines crops growth and production is the leaf area. The yield of a crop depends on the ability of plant canopy to intercept radiation and to convert the energy captured in biomass. The ability of crop to capture light energy can be estimate by the leaf area index (LAI), defined as the ratio of leaf area to a given unit of land area. LAI is related to light interception, crop water balance, crop growth, weed control, crop–weed competition, and soil erosion, therefore, it is highly relevant for many areas of agronomy (Campillo et al., 2010).

There are some studies using crop modeling to estimate LAI of tomato (Heuvelink et al., 2005; Piveta et al., 2007; Campillo et al., 2010; Boote et al., 2012; Küçükönder et al., 2016) and the results have demonstrated that is a good alternative to the use of destructive methods for measuring LAI.

Crop modeling

Mathematical models are used in various scientific fields to make predictions from the simulation of real systems. Crop growth simulation models have become important tools for researchers and growers with the purpose of assisting management and improving production (Boote; Scholberg, 2006). The models help in synthesize the information obtained from various experiments or production fields at diverse locations and provide a way to extrapolating to other regions with different environmental characteristics (Naab et al., 2015; Singh et al., 2016).

Great progress in crop modeling occurred in the decade of 70 when De Wit (De Wit; Goudriaan, 1974 cited by Porter et al., 2010) divided productivity in three levels, in which models should be developed. Potential Production: it is considered

that the culture is adequately supplied with water and nutrients and do not suffer any kind of stress. Its production is only affected by temperature, light, CO^2 concentration and genetic characteristics. Models in this level of productivity help in studies of comparisons with actual productivity to quantify and manage yield gaps; Productivity achievable: in which limitations of water and/or nutrients may occur any time. These models help in the study of lack of rain, irrigation and fertilizer management and soil fertility; Real productivity: at this level, beyond the above limitations, the model incorporates the occurrence of pests and diseases and other causes of stress that may damage the plant tissue and reduce the actual production (Porter et al., 2010).

The crop models can be empirical or mechanistic. The empirical models use correlation and regression analysis to achieve a quantitative knowledge of the process, while mechanistic models include the processes of plant development, such as phenological phases, carbohydrates partitioning, photosynthesis rate, nitrogen and water balance, etc, and provide a better understanding of cause and effect of the processes. Generally mechanistic models are more adaptable for use in different environmental conditions (Sodré, 2007).

Crop models should accurately predict soil water balance, evapotranspiration, and water deficit effects on the processes of development and growth of plants and ultimately yield (Porter et al., 2009). There are a long process to obtain good models, Boote and Scholberg (2006) summarized the process of building a crop model.

> Models should first be calibrated against observed crop growth under conditions where neither water nor nitrogen is limiting. Environmental conditions (light, temperature, CO_2, humidity, wind speed, etc.) for such studies should be monitored while the supply of water and nutrients should be optimized. Environmental conditions, along with management and crop genetic attributes are used as model inputs and then model predicted growth is compared to observed growth and yield. After confirmation of model performance under conditions where development, growth and yield formation are mainly dictated by temperature, CO_2, and solar radiation, models can then be tested under water- and nutrient-limiting conditions. Ultimately, larger scale tests in commercial settings may be required to assess overall model performance and/or robustness of these models (Boote; Scholberg, 2006).

The models are simplifications of a system and so there are some limitations on its use, for example: The complexity of the model should be adjusted to what it was proposed and the results of more complex models are difficult to interpret. The models must be clearly described to avoid the wrong use and interpretation. Obtaining good data is difficult and the model to be used will depend on the available data (Sodré, 2007)

There are some systems that include many crops models such as DSSAT (Jones et al., 2003), AQUACROP (Steduto et al., 2009) and APSIM (McCown et al., 1996). These models are multidisciplinary and use the knowledge in agrometeorology, plant physiology, soil science, etc., to make estimates in order to help growers and researchers. DSSAT is a suite of more than 16 crop models and strategic analysis programs that have been successfully worldwide used (Dzotsi et al., 2010), including the CROPGRO-Tomato model.

There are some models developed for tomato with the purpose of predicting partitioning of dry matter (Zhu et al., 2009), growth and yield response to temperature (Boote et al., 2012), and fruit quality (Teng et al., 2012), leaf area and leaf area index (Heuvelink et al., 2004; Piveta et al., 2007; Campillo et al., 2010; Üçükönder et al., 2016). In spite of that, no models was found for simulations of tomato response to P-fertilization, however some studies have demonstrated the usefulness of mathematical models in the study of P processes in maize (Dzotsi et al., 2010) and peanut (Naab et al., 2015).

In the present study the CROPGRO-Tomato model was improved by parameterization and calibration with data of phosphorus in tomato plants to simulate the response of the culture to P-fertilization. Also it was used crop modeling to estimate leaf area index of tomato plants using no-destructive methods of measuring leaf area, which is a important parameter for mechanistic models, and it was described the patterns of nutrients uptake and biomass accumulation and partitioning during the plant cycle.

REFERENCES

ALVARENGA, M. A. R. Origem, botânica e descrição da planta. In: _____. (Ed.). **Tomate: Produção em campo, casa de vegetação e em hidroponia.** Lavras: UFLA, 2004. p. 13-23.

BOOTE, K. J; SCHOLBERG, J. M. S. Developing, parameterizing, and testing of dynamic crop growth models for horticultural crops. **Acta Horticulturae**, n. 718, p. 23–34, 2006. Available in: < http://dx.doi.org/10.17660/ActaHortic.2006.718.1>

BOOTE, K. J; RYBAK, M. R; SCHOLBERG, J. M; JONES, J. W. Improving the CROPGRO-tomato model for predicting growth and yield response to temperature. **HortScience**, v. 47, n. 8, p. 1038-1049, 2012.

CAMPILLO, C; GARCÍA, M. I; DAZA, C; PRIETO, M. H. Study of a non-destructive method for estimating the leaf area index in vegetable crops using digital images. **HortScience**, v. 45, n. 10, p. 1459-1463, 2010.

DE WIT, C. T; GOUDRIAAN, J. **Simulation of ecological processes**. Centre for Agricultural Publishing and Documentation., 1978.

DZOTSI, K. A; JONES, J. W; ADIKU, S. G. K; NAAB, J. B; SINGH, U; PORTER, C. H; GIJSMAN, A. J. Modeling soil and plant phosphorus within DSSAT. **Ecological Modelling**, v. 221, n. 23, p. 2839-2849, 2010.

FAOSTAT, Food and Agriculture Organization of The United Nations Statistics**. Top 50 Commodities.** 2013. Available in: <http://faostat3.fao.org/browse/rankings/commodities_by_regions/E>. Access:08 sept. 2016.

Heuvelink, E; Bakker, M.J; Elings, A; Kaarsemaker, R.C; Marcelis, L.F.M. Effect of leaf area on tomato yield. **Acta horticulturae**, v. 691, p. 43-50. 2005 DOI: 10.17660/ActaHortic.2005.691.2

IBGE: INSTITUTO BRASILEIRO DE GEOGRAFIA E ESTATÍSTICA. **Levantamento Sistemático da Produção Agrícola.** Rio de Janeiro:IBGE, v.27, n.01 p.1-85, 2016.

JONES, J. W; HOOGENBOOM, G; PORTER, C. H; BOOTE, K. J; BATCHELOR, W. D; HUNT, L. A; WILKENS, P. W; SINGH, U; GIJSMAN, A. J; RITCHIE, J. T. The DSSAT cropping system model. **European journal of agronomy**, v. 18, n. 3, p. 235-265, 2003.

KÜÇÜKÖNDER, H; BOYACI, S; AKYÜZ, A. A modeling study with an artificial neural network: developing estimationmodels for the tomato plant leaf area. **Turkish Journal of Agriculture and Forestry**, v. 40, n. 2, p. 203-212, 2016.

LAHOZ, I; PÉREZ-DE-CASTRO, A; VALCÁRCEL, M; MACUA, J. I; BELTRÁN, J; ROSELLÓ, S; CEBOLLA-CORNEJO, J. Effect of water deficit on the agronomical performance and quality of processing tomato. **Scientia Horticulturae**, v. 200, p. 55-65, 2016.

MCCOWN, R. L; HAMMER, G. L; HARGREAVES, J. N. G; HOLTZWORTH, D. P; FREEBAIRN, D. M. APSIM: a novel software system for model development, model testing and simulation in agricultural systems research. **Agricultural systems**, v. 50, n. 3, p. 255-271, 1996.

NAAB, J. B; BOOTE, K. J; JONES, J. W; PORTER, C. H. Adapting and evaluating the CROPGRO-peanut model for response to phosphorus on a sandy-loam soil under semi-arid tropical conditions. **Field Crops Research**, v. 176, p. 71-86, 2015.

NANGARE, D. D; SINGH, Y; KUMAR, P. S; MINHAS, P. S. Growth, fruit yield and quality of tomato (*Lycopersicon esculentum* Mill.) as affected by deficit irrigation regulated on phenological basis. **Agricultural Water Management**, v. 171, p. 73-79, 2016.

PORTER, C. H; JONES, J. W; ADIKU, S; GIJSMAN, A. J; GARGIULO, O; NAAB, J. B. Modeling organic carbon and carbon-mediated soil processes in DSSAT v4. 5. **Operational Research,** v. 10, n. 3, p. 247-278, 2010.

SANT'ANA, R. R.; NASCIMENTO, A. R. **Perspectivas do setor de tomate industrial.** Available in: <http://www.revistacampoenegocios.com.br/perspectivas-do-setor-de-tomate-industrial/>. Access: 09 sept. 2016.

SILVA, J. D; GIORDANO, L. D. B; FURUMOTO, O., BOITEUX, L. D. S., FRANÇA, F. H., VILLAS-BOAS, G. L. V., ... & ÁVILA, A. C. **Cultivo de tomate para industrialização.** Brasília: Embrapa Hortaliças, 2003. p. Available in:

<http://sistemasdeproducao.cnptia.embrapa.br/FontesHTML/Tomate/TomateIndustrial/index.htm>. Access: 09 sept. 2016.

SILVA, J.; GUEDES, I. M. R.; LIMA, C. E. P. (Ed.). Adubação e Nutrição. In: CLEMENTE, F. M. V. T.; BOITEUX, L. S. **Produção de tomate para processamento industrial.** Brasília: Embrapa, 2012. p. 103-127.

SILVA, E. C; MALUF, W. R. Técnica hidropônica para triagem de genótipos de tomateiro quanto à eficiência de absorção de fósforo. **Horticultura Brasileira**, v. 30, n. 2, 2012.

SINGH, S; BOOTE, K. J; ANGADI, S. V; GROVER, K; BEGNA, S; AULD, D. Adapting the CROPGRO model to simulate growth and yield of spring safflower in semiarid conditions. **Agronomy Journal**, v. 108, n. 1, p. 64-72, 2016.

SODRÉ, U. Modelos matemáticos. **Universidade Estadual de Londrina: Londrina**, 2007.

STEDUTO, P; HSIAO, T; RAES, D; FERERES, E. AquaCrop—The FAO crop model to simulate yield response to water: I. Concepts and underlying principles. **Agronomy Journal**, v. 101, n. 3, p. 426-437, 2009.

TENG, L; CHENG, Z; CHEN, X; LAI, L. Study on simulation models of tomato fruit quality related to cultivation environmental factors. **Acta Ecologica Sinica**, v. 32, n. 2, p. 111-116, 2012.

WPTC: World Processing Tomato Council. **Releases.** Available in: <http://www.wptc.to/releases-wptc.php>. Access: 09 sept. 2016.

ZHU, J. Y.; WEN, X. Z.; LI, Y. L. Simulation of dry matter production and partitioning based on source-sink growth unit in greenhouse tomato. **Acta Ecologica Sinica**, v. 29, n. 12, p. 6527-6533, 2009.

CHAPTER 2 - Adapting the CROPGRO-Tomato Model for Response to Phosphorus Fertilization in Tropical Conditions*

Abstract

Crop models are important tools for researchers and growers with the purpose of assisting management and improving production. Some models have been developed for processing tomato (*Solanum lycopersicum*); however, CROPGRO-Tomato as well as other tomato models does not yet have phosphorus response built in. The objective of this study was to adapt the CROPGRO-Tomato model to simulate response to P fertilization and then to evaluate the model performance for simulating growth and yield of processing tomato. A corollary objective was to evaluate and improve N balance processes in the model. Data from experiments conducted in Brazil during the years 2013 and 2014 were used to calibrate and test the performance of CROPGRO-Tomato model for simulate the response to phosphorus fertilization in tropical conditions. The model performed good simulations of biomass, fruit dry and fresh weight, fruit harvest index, and leaf area index with average relative root mean square error of 24%. The model was able to simulate difference in plant-P concentration and reduction in yield when plants were grown in soil with low phosphorus content. CROPGRO-Tomato model is promising to simulate tomato responses to phosphorus fertilization and can be improved by testing in other environments.

1. Introduction

Crop growth simulation models have become important tools for researchers and growers with the purpose of assisting management and improving production (Boote and Scholberg, 2006). In the 1980's, the establishment of the International Benchmark Sites Network for Agrotechnology Transfer (IBSNAT) resulted in the development of the modeling

*Artigo nas normas da revista Agronomy Journal

package DSSAT (Decision Support System for Agrotechnology Transfer) which is widely used and accepted in agricultural research communities (Uehara and Tsuji, 1998). The DSSAT package includes some generic crop models such as CROPGRO. The CROPGRO model is a mechanistic model that allows the simulation of plant development and growth, along with phenological events and processes of nitrogen balance and water balance of a large range of crops in different production systems (Scholberg, 1996; Boote et al., 1998).

Some models have been developed for processing tomato with the purpose of predicting harvest date (Wolf et al., 1986), loss of production due to weed competition (Kropff et al., 1992), and to help in pest management (Wilson et al., 1987). For greenhouse tomato, Jones et al. (1989) developed TOMGRO, a growth model which is sensitive to environmental variation of temperature, CO_2 concentration, and solar radiation. However, TOMGRO assumes that water and nutrients are not limiting, and it was developed for single-stemmed tomato, with continuous node formation due to the indeterminant development. Therefore, the TOMGRO model is not able to simulate growth and development of semi-determinante field-grown tomato, because of the differences in growth characteristics of greenhouse tomato (Scholberg, 1996).

With the purpose of adapting the CROPGRO model for field-grown tomato, Scholberg (1996) found, in the literature, that growth patterns were similar to that observed for other field crops such as peanut (Boote et al., 1986), and that it was more appropriate to modify the existing CROPGRO-Peanut model to simulate growth and development of field-grown tomato.

Although the CROPGRO-Tomato has been developed for simulation of growth and development of semi-determinate field-grown tomato, it has only been used for experiments and fields that use mulched production beds under optimum water and N fertilization (Rybak,

2009). Boote and Scholberg (2006) emphasized the importance of calibrating and testing models by comparison to measured data in real field situations where water or nitrogen are not limiting, in order to adapt the model for simulation under typical system and environments. However, the model has not been tested for true open fields lacking plastic mulched beds, where the water and N balance are subjected to dramatic rainfall-induced fluxes, as well as having soil surface water evaporation.

Another important issue related to producing tomato is the field characteristics. Field-grown tomato can be affected by soil natural P concentration and would respond to P fertilization, but the CROPGRO-Tomato model does not yet have P response built in. It is known that P is a nutrient that provides significant yield increases for tomato production, when tomato is grown on highly weathered soil under tropical conditions (Silva and Maluf, 2012). In recent research, Naab et al. (2015) used a generic soil and plant P module coded for DSSAT v4.5 crops to parameterize CROPGRO-Peanut for response to P fertilization under P-infertile soils. However, as far as we are aware, no work has been done to adapt CROPGRO-Tomato model for response to P fertilization and soil P infertility.

Thus the objective of this study was to adapt the CROPGRO-Tomato model to simulate response to P fertilization, and test the ability of the model to simulate growth, development, and yield of field-grown tomato. A corollary objective was to evaluate and improve N balance processes in the model, because the model has not been previously simulated with N balance processes turned “on”, since all prior evaluations were conducted under plastic mulch bed systems in which N leaching was not simulated.

2. Materials and Methods

2.1 Experiments for model calibration and testing

The data for model calibration were collected in three field experiments (EC1, EC2, EC3) and for testing in two field experiments (ET1 and ET2) conducted in the rural area of Guaíra city, in the state of São Paulo-Brazil (20º27'S lat; 48º19'W long), but in different sites (Table 1). The climatic classification is tropical with dry winter (Köppen = Aw; Thornthwaite = B_1rA'a'), and the annual average rainfall is 1374 mm. The soil at the experimental sites is classified as Typic Hapludox (highly weathered deep clay soil), with average 52% clay, 29% silt, and 19% sand. Samples were taken from 0-20 cm depth for soil chemical characterization (Table 2).

Table 1. Description of field experiments used for calibration and testing of CROPGRO-Tomato model.

Experiment	Initial Soil Condition	Doses of P (kg ha^{-1})	Transplant Date	Harvest Date
		Calibration		
EC1	High P content	65, 131, 192, 262, 328	29 Apr. 2013	06 Sep. 2013
EC2	Low P content	87, 175, 262, 350, 437	14 June 2013	07 Oct. 2013
EC3	High P content	87, 175, 262, 350, 437	26 May 2014	23 Sep. 2014
		Testing		
ET1	High P content	196	29 Apr. 2013	06 Sep. 2013
ET2	Low P content	196	08 Mar. 2013	06 July 2013

After plowing and harrowing of the area, rows were opened and urea and KCl were applied at a dose equivalent to 30 kg ha^{-1} of N and 50 kg ha^{-1} of K (Trani et al, 1997). The treatments of ECs consisted of five P doses provided by application of Triple Super Phosphate (Table 1). Each EC experiment also had one control treatment (without P application). For both ET1 and ET2 phosphorus fertilization was equivalent to 196 kg ha^{-1}. Following the fertilization, mechanized planting of seedlings was done.

Table 2. Soil chemical characteristics in the 0-20 cm depth at experimental sites.

Experiment	P resin	OM	pH	K	Ca	Mg	H+Al	SB[†]	CEC[††]	V[†††]
	mg dm^{-3}	g dm^{-3}	($CaCl_2$)	----------mmol$_c$ dm^{-3} ----------						%
EC1 and ET1	116	29	5.6	3.5	28	6	29	37	66	57
EC2 and ET2	19	26	4.5	1.1	8	6	36	15	51	30
EC3	122	15	5.9	4.2	70	22	20	96	116	83

[†] Sum of bases (K+Ca+Mg);
[††] Cation Exchange Capacity;
[†††] Bases Saturation (percentage of CEC filled by K, Ca, and Mg).

For top dressing 30 kg ha^{-1} of N was applied at 30 days after transplanting (DAT) and again at 50 DAT, also 133 kg ha^{-1} of K was applied divided in three applications at 45, 65 and 85 DAT.

The cultivar of processing tomato used in all experiments was Heinz-9553. The age of seedlings at time of transplanting was adjusted to match phase duration since the real age was not available. The criterion for the adjustment was the knowledge that the usual age of tomato seedlings for transplanting in this region is about 3 wk.

The transplant of seedlings was established in row space 1.25 m and the plants were spaced 0.25 m from each other. In ECs, the treatments were replicated four times using randomized block design, totaling 24 plots. Each plot had three rows of 6 m (22.5 m^2), but only the central row was used for plant evaluations. For the ET1 and ET2 no plots were used. Ten plants collection times was adopted. The plants were collected randomically in four sampling points within the area, representing four replication with four plants each.

The crop was weekly irrigated by center pivot with application of 25 mm of water from transplanting to early flowering and 40 mm from flowering to five days before harvest, always discounting rainfall during the period.

For evaluation of ECs, one plant per plot was collected at 15, 30, 45, 60, 75, 90, 105, and 120 days after transplanting (DAT) to measure the leaf area using Li-Cor (LI-3100C Area Meter) and to determine biomass of shoot and fruits. Leaf area was used for calculating the

leaf area index (LAI), that represents the area of leaves per area of land. To determine biomass, the whole plants were washed, separated in fruits and shoot (leaves+stem), dried at ±65 ºC until constant mass, then weighed.

At beginning flowering (about 50 DAT), 10 samples of the fourth fully developed leaf from the tip of the branch were collected in each plot of ECs for determination of N and P content in plant. The samples were washed, dried at ±65 ºC, and ground separately in a Wiley mill (20 mm sieve), then subsamples were subjected to acid digestion to determine N and P concentration (AOAC, 1990). The values obtained for N and P content were multiplied by the plant biomass from same sample date to determine the amount of nutrient accumulated.

The plants from ET1 and ET2 were collected at 30, 40, 50, 60, 70, 80, 90, 100, 110, and 120 DAT. Plants were washed and divided in vegetative parts (leaves + stems) and reproductive (fruit), then dried in an oven with forced air circulation at ±65 °C until constant mass to obtain biomass of fruits and total. Also subsamples were used to determine P accumulated in vegetative and reproductive parts of plants as describe above.

Weather data of maximum and minimum air temperature (ºC), rainfall (mm), wind speed (m s^{-1}), solar irradiation (MJ $m^{-2}d^{-1}$), and relative humidity (%) were measured daily by an automatic weather station Campbell Scientific 21X Micrologger® located at the experimental sites.

2.2 Model input data

The information from the weather station was input into DSSAT V4.6 with data collected from Apr. 2013 to Sept. 2014 using the Weatherman tool. Also three soil profiles, corresponding to each experimental site, had to be created using SBuild, along with soil chemical and textural characteristics to parameterize soil initial conditions of each experiment. The missing data of organic carbon in deeper layers (20 cm to 100 cm) were

estimated by the default equation of DSSAT- Century model (Parton et al, 1994) using soil texture.

To initialize the soil organic matter (SOM) in each experiment the default regression equation of the model was used, following these steps: First, measured organic carbon was entered in the Soil Analysis and the stable carbon was computed by using the default regression. Then the model was run one time starting considerably prior to planting to simulate the inorganic nitrogen concentrations of respective layers on the day of planting (available in SoilNi.OUT file). These values were set as initial conditions in the soil profile for the concentrations of ammonium and nitrate in soil layers.

All the data on climate, soil, crop growth, management, and yields collected in five experiments were entered in the standard DSSAT files (*.TMX, *.TMA, *.TMT, *.WTH, *.SOL) needed for execution of the CROPGRO-Tomato model.

2.3 Calibration of cultivar

The CROPGRO-Tomato model required calibration of genetic coefficients in the cultivar file since a new cultivar was used for the experiments. These coefficients describe durations of developmental phases of a specific cultivar.

For calibration of cultivar Heinz-9553 data from ECs were used and also the coefficients of cultivar Solarset, already in the cultivar file, with similar life cycle duration, were used as a starting point.

Overall, the changes in Heinz-9553 cultivar coefficients made life cycle shorter than Solarset. For the vegetative phase, EM-FL (time between plant emergence and flowering) was decreased by four photothermal days (PTD) to reach earlier flowering and fruit set. After the initialization of fruit production, the time between first seed and physiological maturity (SD-PM) was reduced from 47 to 42 PTD to reduce this phase duration. The coefficient PODUR

(duration of fruit addition) was reduced by two PTD from 56 to 54, and XFRT (maximum fraction of daily growth partitioned to fruit) was decreased from 0.78 to 0.73, in order to improve simulation of fruit growth and fruit harvest index (HI).

Other changes in Heinz-9553 coefficients were the reduction in FL-LF (time between first flower and end of leaf expansion) from 47 to 38 PTD, and in SLAVR (specific leaf area of cultivar) from 300 to 230 cm^2 g^{-1}. These changes resulted in reduction of leaf size and dry mass, and were performed to improve leaf area index (LAI) simulations. The genetics coefficients of Solarset (starting point) and of cultivar Heinz-9553 after calibration are shown on Table 3.

Table 3. Genetic coefficients of cultivar Heinz-9553 after calibration, compared to starting point cultivar (Solarset).

Genetic Coefficient	Abbreviation	Solarset	Heinz-9553
Critical Short Day Length below which reproductive progresses with no daylength effect development (for short day plants) (hour)	CSDL	12.33	12.33
Slope of the relative response of development to photoperiod with time (positive for short day plants) (1per hour)	PPSEN	0	0
Time between plant emergence and flower appearance (R1) (photothermal days)	EM-FL	31	27
Time between first flower and first fruit (R3) (photothermal days)	FL-SH	4.6	4.5
Time between first flower and first seed (R5) (photothermal days)	FL-SD	21	21
Time between first seed (R5) and physiological maturity (R7) (photothermal days)	SD-PM	47	42
Time between first flower (R1) and end of leaf expansion (photothermal days)	FL-LF	47	38
Maximum leaf photosynthesis rate at 30 ºC, 350 vpm CO_2, and high light (mg CO_2 m^{-2-s})	LFMAX	1.36	1.36
Specific leaf area of cultivar under standard growth conditions (cm^2 g^{-1})	SLAVR	300	230
Maximum size of full leaf (three leaflets) (cm^2)	SIZLF	300	300
Maximum fraction of daily growth that is partitioned to seed + shell	XFRT	0.78	0.73
Maximum weight per seed (g)	WTPSD	0.004	0.004
Seed filling duration for fruit cohort at standard growth conditions (photothermal days)	SFDUR	27	26
Average seed per fruit under standard growing conditions (number per fruit)	SDPDV	300	300
Time required for cultivar to reach final fruit load under optimal conditions (photothermal days)	PODUR	56	54
Threshing percentage. The maximum ratio of (seed/(seed+shell)) at maturity. Causes seed to stop growing as their dry weight increases until the shells are filled in a cohort	THRSH	8.5	8.5
Fraction protein in seeds (g(protein) g^{-1}(seed))	SDPRO	0.3	0.3
Fraction oil in seeds (g(oil) g^{-1}(seed))	SDLIP	0.05	0.05

2.4 Model description

The DSSAT - P model has two soil modules, inorganic P and organic P, and one plant P module. The inorganic soil P module simulates transformations among labile P, active P, and stable P pools that occur in two volumes of soil: 1) non-root zone (volume that is not in direct contact with roots), and 2) a root zone that is in contact with roots within ROOTRAD radius (mm) of each root, associated with root length density in each soil layer, where ROOTRAD = radius of P extraction distance from the root surface. ROOTRAD can be considered a proxy for root hair influence away from the root.

Organic soil P module simulates transformation occurring among four SOM pools (active, slow, passive, and fresh). Phosphorus mineralization and immobilization depend on the amount of organic P and C flowing from one SOM pool to another and the C/P ratio of receiving pool.

In the plant P module, optimum (=critical) and minimum P concentration over the crop life cycle are set in the species file for different plant organs progressing from three successive developmental phases: emergence, first flower, and full seed.

2.5 Calibration of parameters in species file

In the species file, parameters of the processes related to plant development and growth, and the plant sensitivity to environmental conditions, such as temperature, CO_2 concentration, water stress, P status, N status, etc., are defined. The species file also includes coefficients of plant composition and partitioning.

The optimum P concentration at any developmental phase of the plant is the minimum concentration required to obtain maximum growth rate. If P concentration at any phase of crop cycle drops below P optimum there is a deficit and may induce a plant response to P stress limitation (Naab et al., 2015). There are two types of P stresses possible, first, the stress

reduction of photosynthesis (SRATPHOTO) and secondly the stress modification of partitioning of assimilate to roots (SRATPART). As parameterized for the CROPGRO-Peanut model by Naab et al. (2015), the stress reduction of partitioning to root should occur somewhat sooner (at ratio of 0.83) than does the reduction in photosynthesis (0.63). Another important parameter on P partitioning is the FracPMobil that represents the maximum fraction of P which can be mobilized per day from leaf and stem (0.20).

The P optimum and minimum concentration in shoot, root, and fruit of tomato at emergence, first flower, and full seed were set from literature data (Besford ,1979; Bryla and Koide, 1998; Alvarez V et al., 2002; and Demir et al., 2010) and also from ECs experiments, where neither water nor nitrogen were limiting. The mean values were 3.4 g $kg^{-1}$for P concentration in shoot at starting flowering and 1.8 g kg^{-1} full seed phase. These values were used as starting point to guide the initialization of P parameters (Fig. 1), then calibrations were made iteratively of these P concentration targets to better simulate the actual P concentration in shoot and in fruits. ROOTRAD also was calibrated in order to improve simulated tomato plant growth, yield reductions, and P uptake under P limitation. The calibrated parameters of optimum and minimum P concentration and ROOTRAD are shown in Table 4.

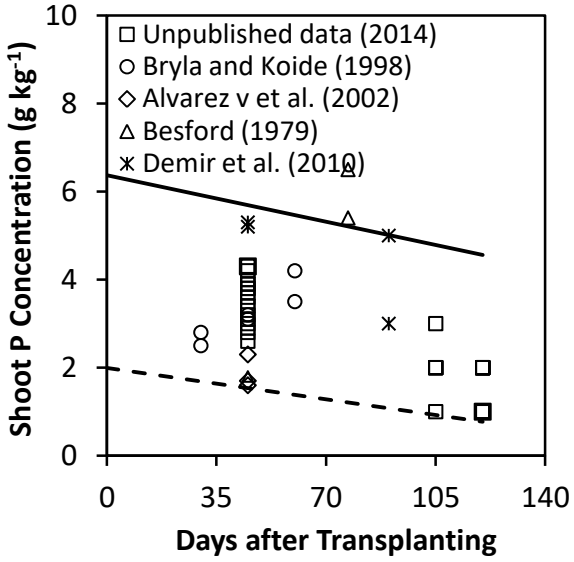

Figure 1: Tomato vegetative (leaves+stem) P concentration variation with time in different experiments.

Table 4. (a) Optimum and minimum P concentration in different plant parts at successive growth stages, and (b) ROOTRAD‡ parameter, after calibration and as used in the P module for tomato.

Growth stage		Emergence	1st flower	Full seed
(a) Plant part		----------g kg^{-1}----------		
Leaf	Optimum	5.5	3.7	2.5
	Minimum	3.0	2.0	1.0
Stem	Optimum	5.5	3.7	2.5
	Minimum	3.0	2.0	1.0
Root	Optimum	5.5	3.7	2.5
	Minimum	3.0	2.0	1.0
Shell	Optimum	-	5.5	4.7
	Minimum	-	3.5	2.5
Seed	Optimum	-	5.5	4.7
	Minimum	-	3.5	2.5
(b) Parameter	Value	Definition		
‡ROOTRAD	0.0054	Radius (m) of cylinder around roots from which soil P can be extracted.		

However, for the purposes of the present study, the N balance was, for the first time, turned on, therefore calibration/adjustments of some parameters related to N balance, such as NMOBMX, NVSMOB, and SENRTE, were needed to improve the simulations (Table 5), and P balance parameterization had to be created.

Table 5. Genetic coefficients of tomato species file, original (V4.5 CROPGRO-Tomato) and newly-calibrated, related to N mobilization and leaf senescence.

Coefficient	Abbreviation	Original	Calibrated
Maximum fraction of N that can be mobilized per day.	NMOBMX	0.09	0.13
Relative N mobilization rate in vegetative phase, relative to reproductive phase.	NVSMOB	0.38	0.93
Senescence rate (g. mass of "exhausted leaf" abscised per g. of protein mobilized)	SENRTE	1	2.50

2.6 Statistical Evaluation

After parameterization and calibration, the simulated data were compared with the observed data using model evaluation statistics as described by Singh et al. (2016). The Willmott Agreement Index (*d*) (Willmott et al., 1985) measures the agreement between simulated and observed data. It is calculated using the equation:

$$d = 1 - \left[\frac{\sum_{i=1}^{n} Pi - Oi^2}{\sum_{i=1}^{n} (|Pi'| + |Oi'|)^2} \right] \quad 0 \le d \le 1$$

Where: n is the number of observations, P_i is the predicted value for the ith measurement, O_i is the observed value for the ith measurement, $\bar{O}$ is the overall mean of observed values, and $P_i' = P_i - \bar{O}$ and $O_i' = O_i - \bar{O}$. The index varies between 0 and 1, with a value of 1 indicating perfect agreement between predicted and observed data.

The other evaluation statistic used was the relative root mean square error (RRMSE), which is calculated using the equation:

$$RRMSE = \frac{\sqrt{\sum_{i=1}^{n} (Pi - Oi)^2 / n}}{\mu}$$

Where: n is the number of observations, P_i is the predicted value for the ith measurement, O_i is the observed value for the ith measurement, and μ is the mean of all observed values. The

RRMSE is always positive and when equal to 0 indicates perfect agreement between observed and predicted data.

3. Results and Discussion

The CROPGRO-Tomato model was calibrated using ECs for simulations of above-ground biomass, fruit dry weight, fruit fresh weight, fruit harvest index (HI), leaf area index (LAI), nitrogen concentration, and also P optimum, minimum and actual concentration in vegetative tissue (leaf +stem) and in fruits. For testing the capability of model in simulate the response of tomato to P fertilization comparisons between observed data of ETs and simulated values were made.

3.1 Growth and production parameters

Model simulations for above-ground biomass, fruit dry weight and fruit fresh weight after calibrations suggest that tomato is not responsive to P doses when P content in soil is high (Figs. 2a, 3a, 4a and 2c, 3c, 4c).

The model was able to simulate different response of tomato grown in soil with low P concentration when P fertilizer was not applied (Figs. 2b, 3b, and 4b). The RRMSE and *d* index for biomass simulation of treatment without P fertilization in EC2 were 0.29 and 0.97, respectively. The model simulated difference in biomass production between the treatment without P compared to the P-fertilized treatments.

In general, above ground biomass was fairly well simulated for all ECs (Fig. 2). On average, the *d* index of the three experiments was 0.96, and RRMSE was 0.28 indicating good performance of the model. However, average biomass of all sampling dates was under-estimated. A summary of observed and simulated means, and also RRMSE and *d* index, for ECs are presented in Table 5.

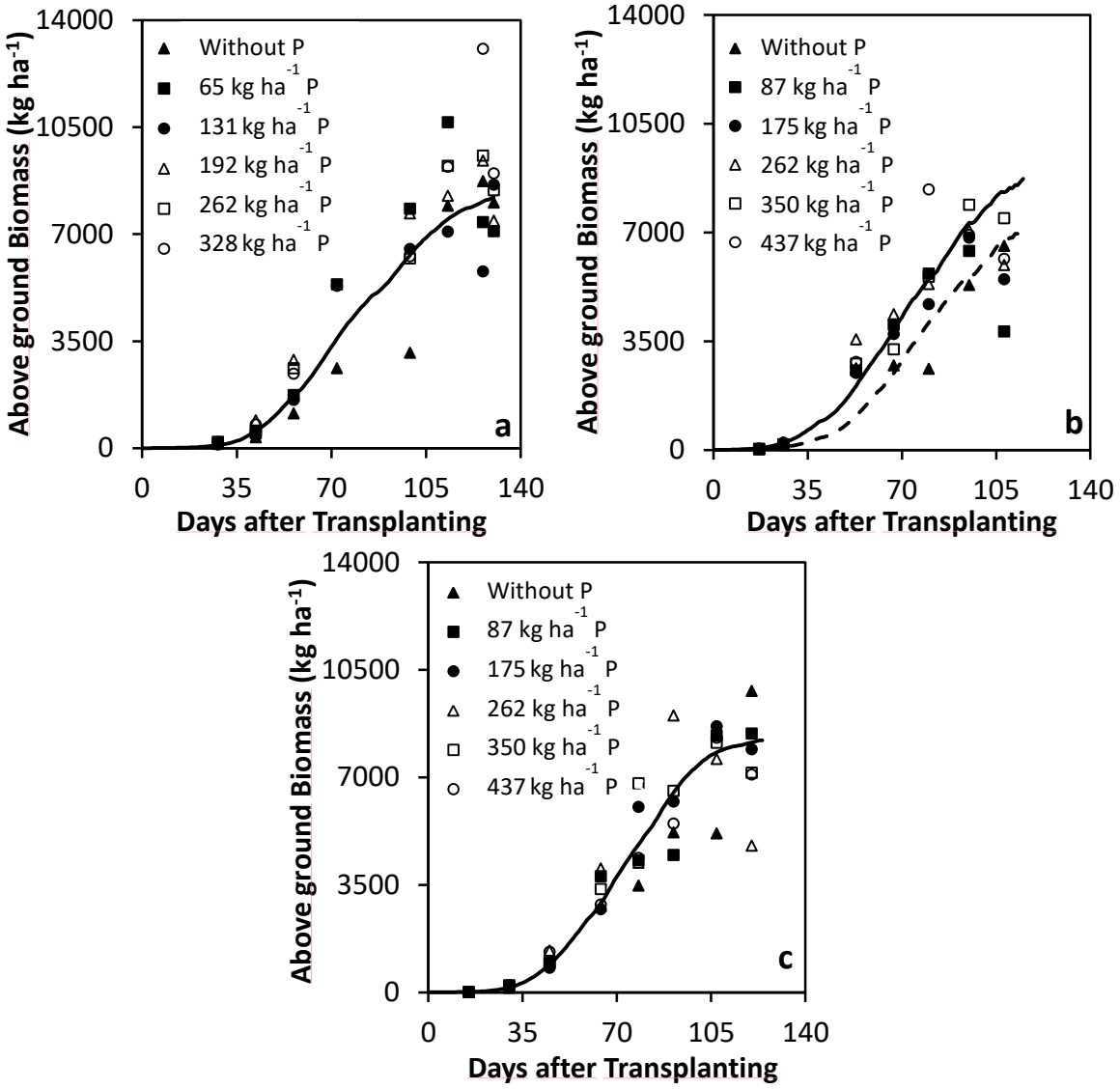

Figure 2. Observed (symbols) and simulated (lines) of tomato above ground biomass production (kg ha^{-1}) in response to doses of P. (a) EC1 (High P); (b) EC2 (Low P); (c) EC3 (High P). Black line: doses of P; Dashed line: without P application.

The simulation of fruit dry weight did not show difference among treatments in EC1 and EC3 (Figs. 3a and 3c). The model over-predicted dry weight of EC1 and EC3, through the season. The simulation showed difference in fruit dry weight of EC2 (Fig. 3b) for the treatment without P fertilization (d = 0.97; RRMSE = 0.21), however, the model under-predicted fruit dry weight of EC2. The average of d index and RRMSE of fruit dry weight simulations of ECs were 0.89, and 0.27, respectively.

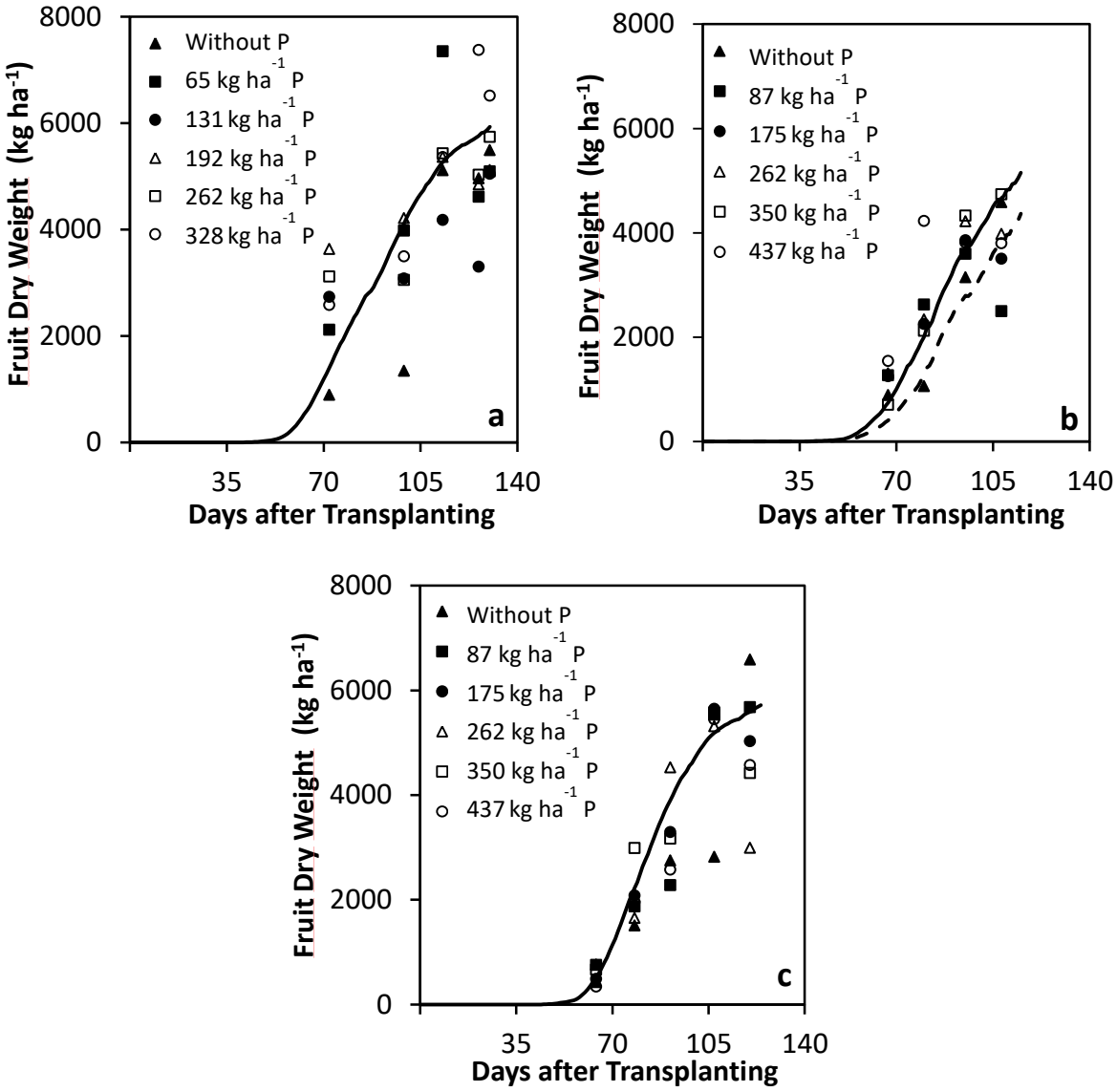

Figure 3. Observed (symbols) and simulated (lines) of tomato fruit (dry weight) production (kg ha^{-1}) in response to doses of P. (a) EC1 (High P)); (b) EC2 (Low P); (c) EC3 (High P). Black line: doses of P; Dashed line: without P application.

The model simulated production of fresh weight of fruit very well in EC1 and EC3. Difference in fresh fruit production was simulated in EC2 (Fig. 4b). The model over-predicted fresh fruit production of EC2, mainly for the treatment without P.

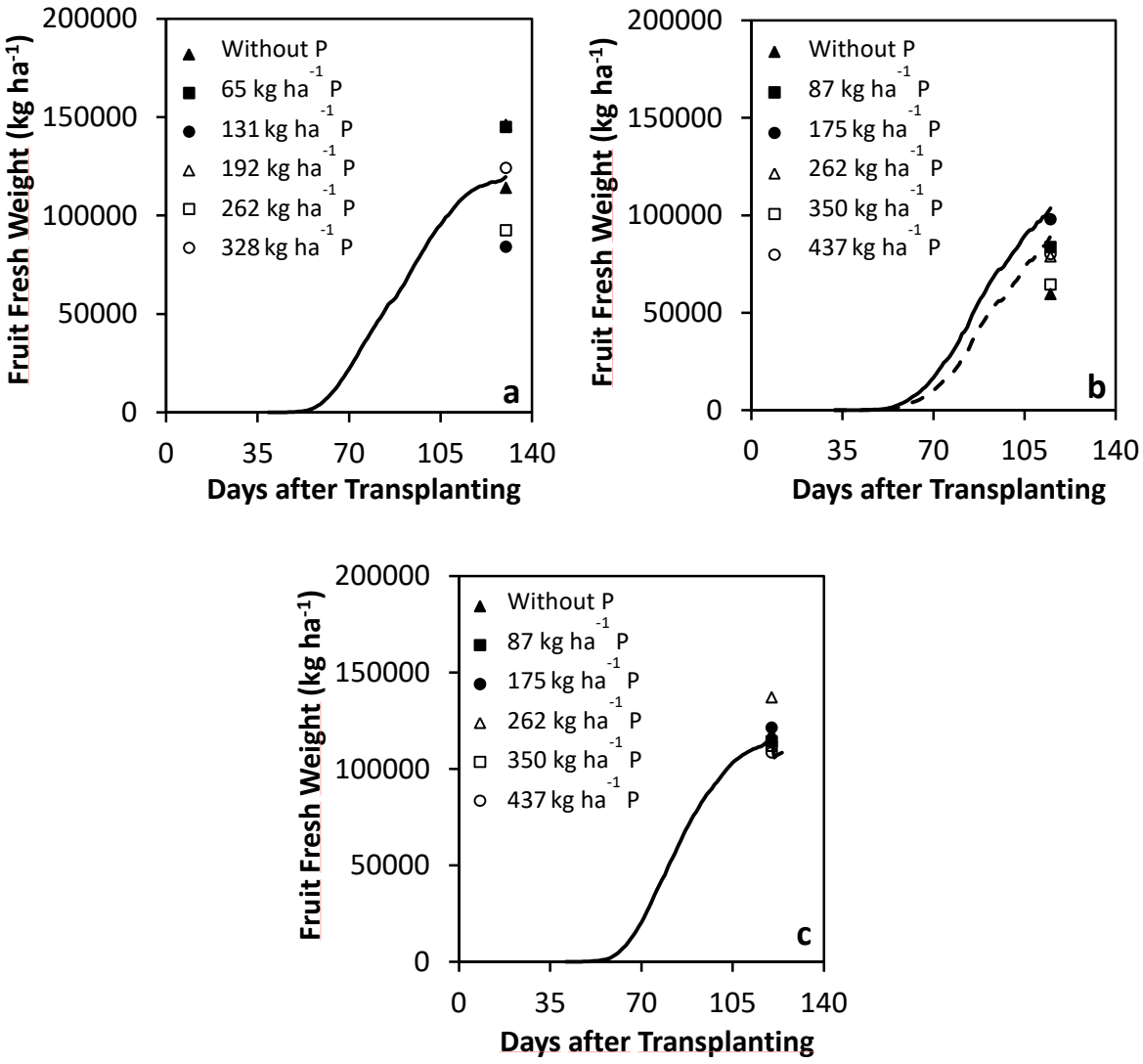

Figure 4. Observed (symbols) and simulated (lines) of final tomato fruit (fresh weight) production (kg ha^{-1}) in response to doses of P. (a) EC1 (High P); (b) EC2 (Low P); (c) EC3 (High P). Black line: doses of P; Dashed line: without P application.

Environmental conditions may have caused some of the differences between simulated and observed fresh fruit production. Boote et al. (2012), in a extensive review of literature, showed temperature as a principal factor that determines fruit-set, the duration of fruit growth period and life cycle of tomato plants. In fact, the temperature during the reproductive phase (first seed to physiological maturity) in EC2 was, on average, 2.5 ºC higher than in EC1 conducted in the same year (2013) (Table 6), which caused the life cycle of plants to be

shorter for EC2 (115 d) than for the EC1 (130 d) and EC3 (124 d). The cause of this difference is that EC2 was planted late in the season (middle of June) compared with the usual date of planting in the region, which is usually late April to middle of May. It is known that tomato fruits are more sensitive to elevated temperatures in both early and late stages of fruit growth, and it may cause loss of fruit-set or production of smaller fruit (Rybak, 2009), however it is impossible to make affirmations if this was one of the reasons causing low fresh fruit weight production, or if it was consequence of short fruit filling duration due the short plant life cycle, because fruit size and fruit number were not measured in the present study.

Table 6. Average temperature and solar radiation during growing phases of tomato plants of experiments for calibration the model.

Growing Phase	First Flower to First Seed				
Experiment	Phase duration (days)	Temperature Max. (ºC)	Temperature Min. (ºC)	Temperature Mean (ºC)	Solar Radiation (MJ m^{-2} d^{-1})
EC1	28	28.9	12.6	20.7	13.1
EC2	34	29.6	8.6	19.1	15.1
EC3	29	27.3	12	19.6	15.1
Growing Phase	First Seed to Physiological Maturity				
Experiment	Phase duration (days)	Temperature Max. (ºC)	Temperature Min. (ºC)	Temperature Mean (ºC)	Solar Radiation (MJ m^{-2} d^{-1})
EC1	69	30.5	9.5	20.0	15.8
EC2	55	32.5	12.6	22.6	18.0
EC3	59	31.9	13.9	22.9	20.9
Growing Phase	Planting to Harvest				
Experiment	Phase duration (days)	Temperature Max. (ºC)	Temperature Min. (ºC)	Temperature Mean (ºC)	Solar Radiation (MJ m^{-2} d^{-1})
EC1	130	29.5	11.4	20.5	15.0
EC2	115	31.1	11.2	21.1	16.1
EC3	124	29.9	13.4	21.7	17.8

Biomass partitioning among plant organs is crucial to economic yield production. The harvest index (HI) is the ratio of total dry mass in the harvested part of plant over the total biomass produced by the plant. The genetic coefficient XFRT determines the fraction of daily dry matter production that will be daily partitioned to the fruits. By reducing this coefficient it was possible to reduce the slope of curve and improve the simulation of fruit HI. The

coefficient PODUR also was calibrated. This coefficient represents the duration of the fruit addition period, and a smaller PODUR makes the start of curve earlier and to rise more sharply. These calibrations improved the simulation of HI of EC1 and EC3 (Fig. 5a and 5c).

The opposite statistics were observed for EC2 (Fig 5b), due XFRT and PODUR calibrations. However, over all EC the RRMSE remained still low and *d* stat high (Table 7). It is important to remember that all calibrations are made iteratively and the effect on simulations of three experiments should be evaluated together in order to make the best decision.

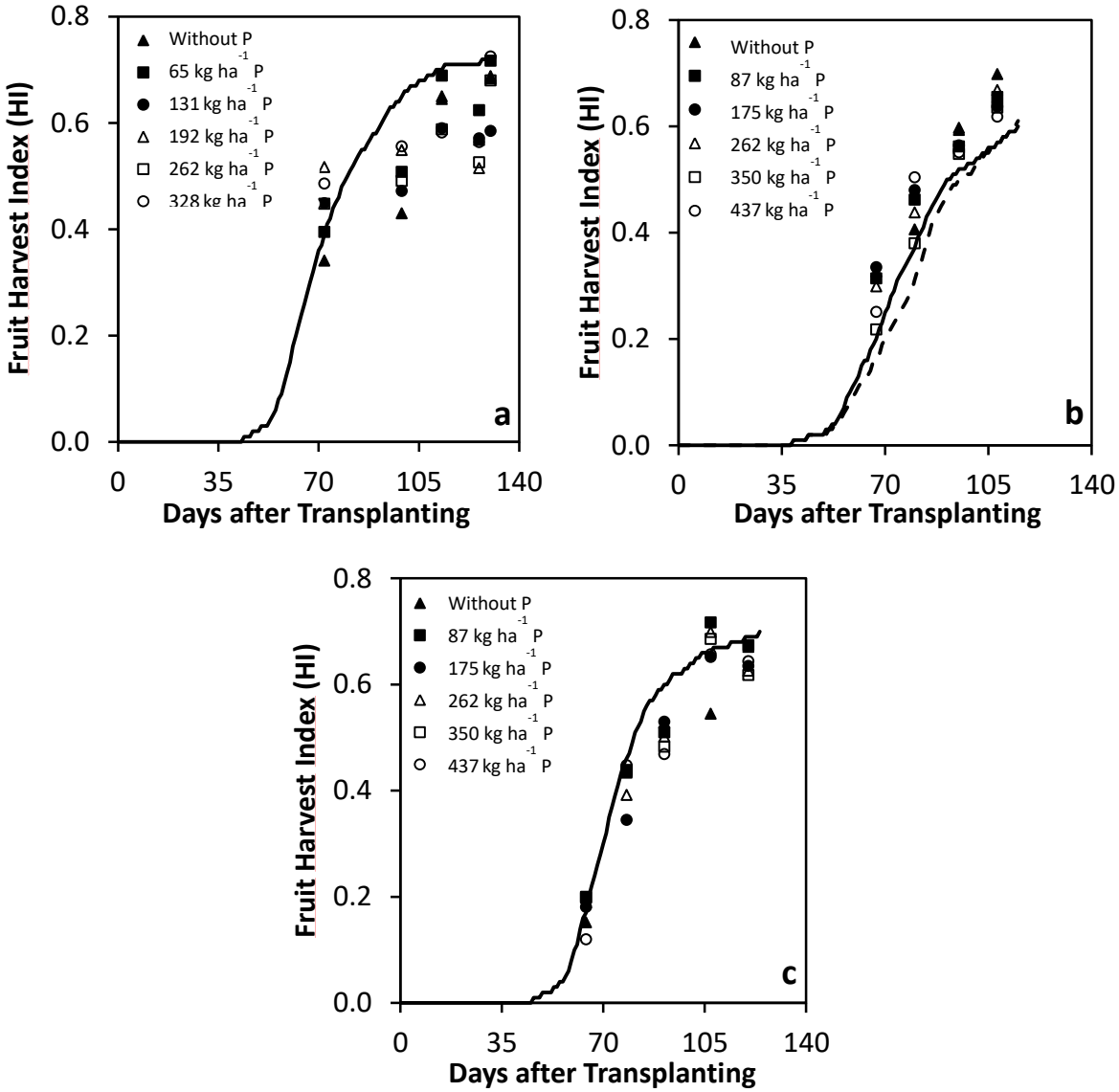

Figure 5. Observed (symbols) and simulated (lines) fruit harvest index of tomato in response to doses of P. (a) EC1 (High P); (b) EC2 (Low P); (c) EC3 (High P). Black line: doses of P; Dashed line: without P application.

The simulations of above ground biomass, fruit dry weight and HI of ETs were highly accurate (Figure 6). That indicates the capability of model in simulate growth and fruit production of field-grown tomato in soil with high and low P content under tropical conditions.

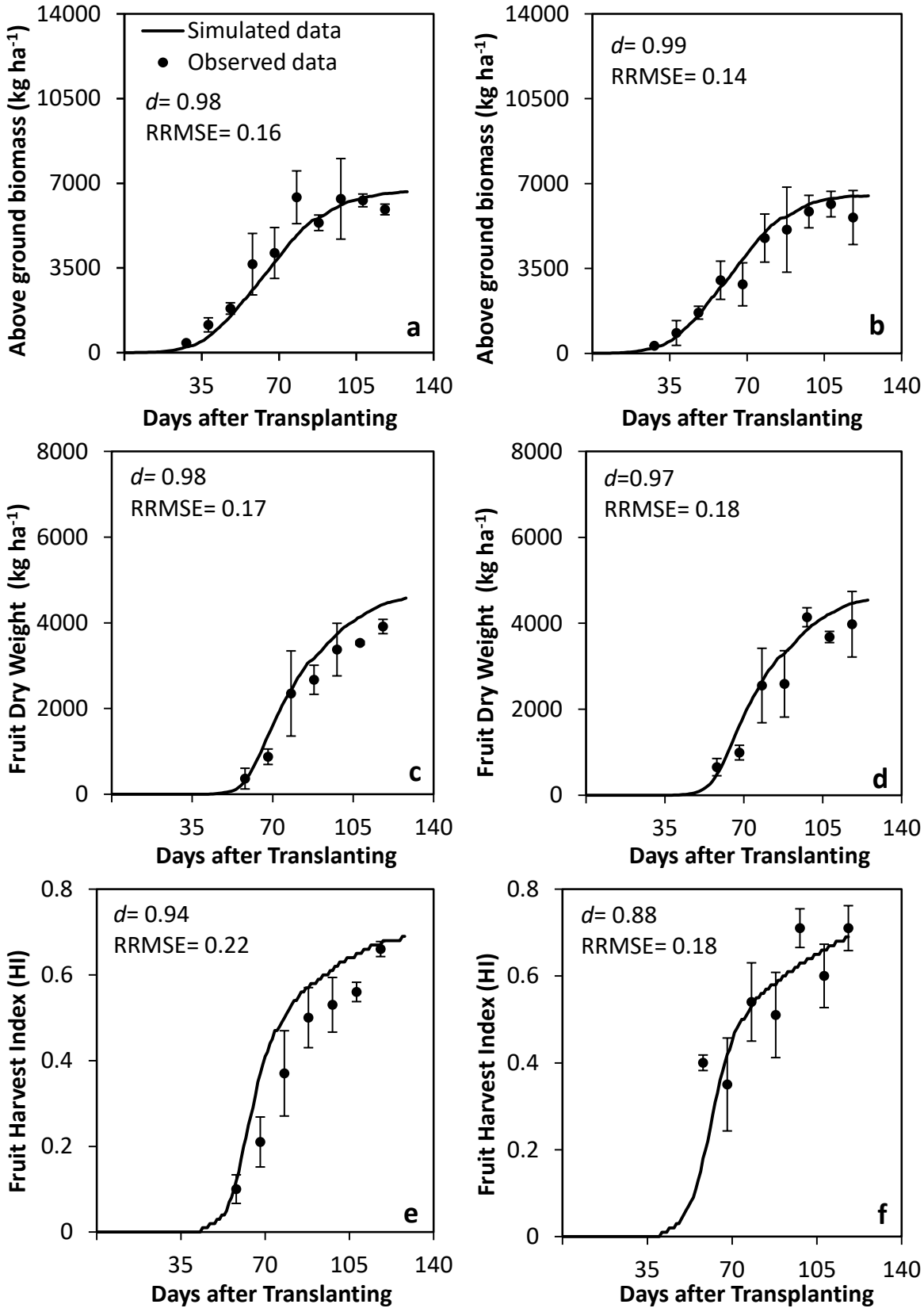

Figure 6. Observed (symbols) and simulated (lines) tomato above ground biomass (kg ha^{-1}) (a, b); fruit dry weight (kg ha^{-1}) (c, d); fruit harvest index (HI) (e, f).
a, c, e: Experiment for testing 1 (ET1); b, d, f: Experiment for testing 2 (ET2).

Table 7. Observed and simulated mean of growth traits for six treatments (mean is averaged over all sampling dates), and their relative root mean square error (RRMSE) and *d* index for time series data.

Crop variable	Experiment	Observed mean	Simulated mean	RRMSE	*d*
Above-ground Biomass (kg ha^{-1})	EC1	5,061	4,503	0.29	0.95
	EC2	3,587	3,732	0.32	0.95
	EC3	3,873	3,901	0.24	0.97
Dry weight of fruits (kg ha^{-1})	EC1	4,339	4,492	0.27	0.83
	EC2	2,820	2,701	0.26	0.89
	EC3	3,156	3,477	0.26	0.94
Fresh weight of fruits (kg ha^{-1})	EC1	117,652	119,603	0.18	-
	EC2	77,453	102,951	0.33	-
	EC3	118,658	115,147	0.06	-
Fruit Harvest Index (HI)	EC1	0.56	0.63	0.20	0.75
	EC2	0.49	0.40	0.17	0.91
	EC3	0.48	0.52	0.13	0.97
Leaf Area Index (LAI)	EC1	1.01	1.04	0.29	0.93
	EC3	1.04	1.04	0.40	0.88

3.2 . Leaf area index (LAI) and nitrogen concentration in vegetative tissues

Some researchers have shown the weaknesses of the model to simulate observed LAI (Rybak, 2009; Boote et al., 2012). Overall, the early growth is well simulated, but later in the season, after maximum leaf area is attained, when leaf area starts declining due to N mobilization and senescence, the model did not reproduce properly the decrease in leaf area.

To improve the simulation of LAI, the NMOBMX and NVSMOB parameters were increased (Table 5) to mimic more rapid yet reasonable decline in N concentration over time as well as sufficiently rapid leaf area decline during reproductive growth to the end of season. These two parameters determine the rate of remobilization of protein from vegetative to reproductive tissues. By increasing these rates, leaf mass declines more rapidly as a result of senescence and N mobilization. Another parameter calibrated to improve LAI simulation was

senescence rate (SENRTE), which controls the intensity of leaf loss per unit of protein mobilized. The RRMSE was reduced from 0.6 to 0.3 in EC1 and from 0.56 to 0.4 in EC3. The *d* index was increased from 0.75 to 0.93 in EC1 and from 0.78 to 0.88 in EC3, for LAI simulation after calibrations (Fig. 7).

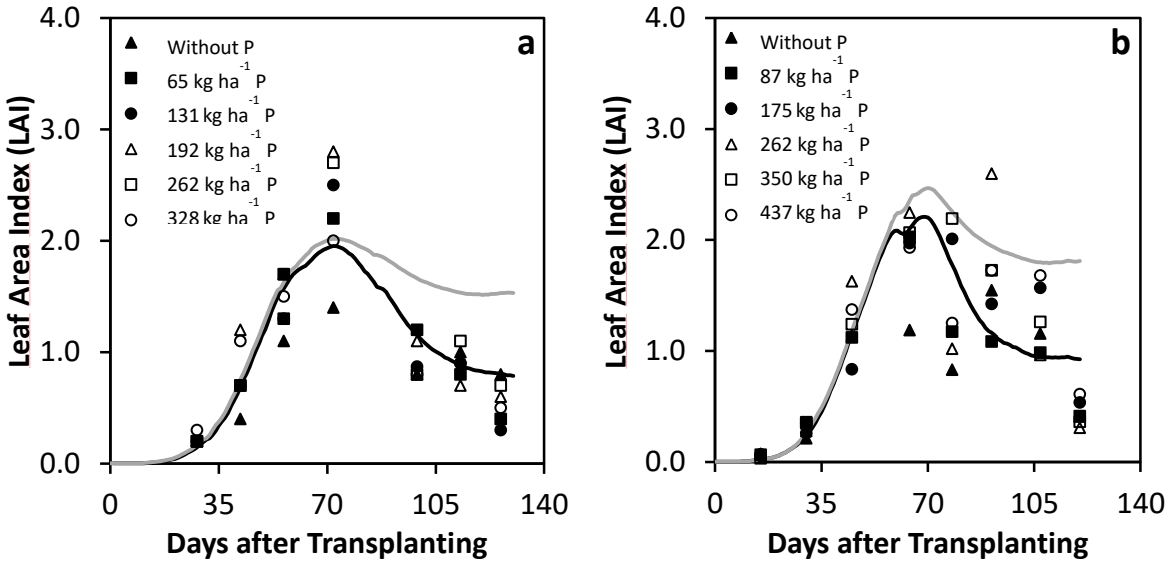

Figure 7. Observed (symbols) and simulated (lines) leaf area index (LAI) of tomato plants in response to doses of P. (a) EC1 (High P); (b) EC3 (High P). Black line = Calibrated (NMOBMX, NVSMOB, SENRTE) for tomato; Gray line = The original parameterization for tomato (DSSAT V4.5).

The observed leaf N concentration at start of flowering in all treatments of ECs ranged from 31 to 56 g kg^{-1}, values close to those (37-42 g kg^{-1}) found by Demir et al. (2010) and Lima et al. (2011) (37-40 g kg^{-1}) in the same growth phase. The recommended N concentration for industrial tomato in early reproductive phase ranges from 40 to 60 g kg^{-1} (Fontes, 2000), where concentrations between these values means no N stress.

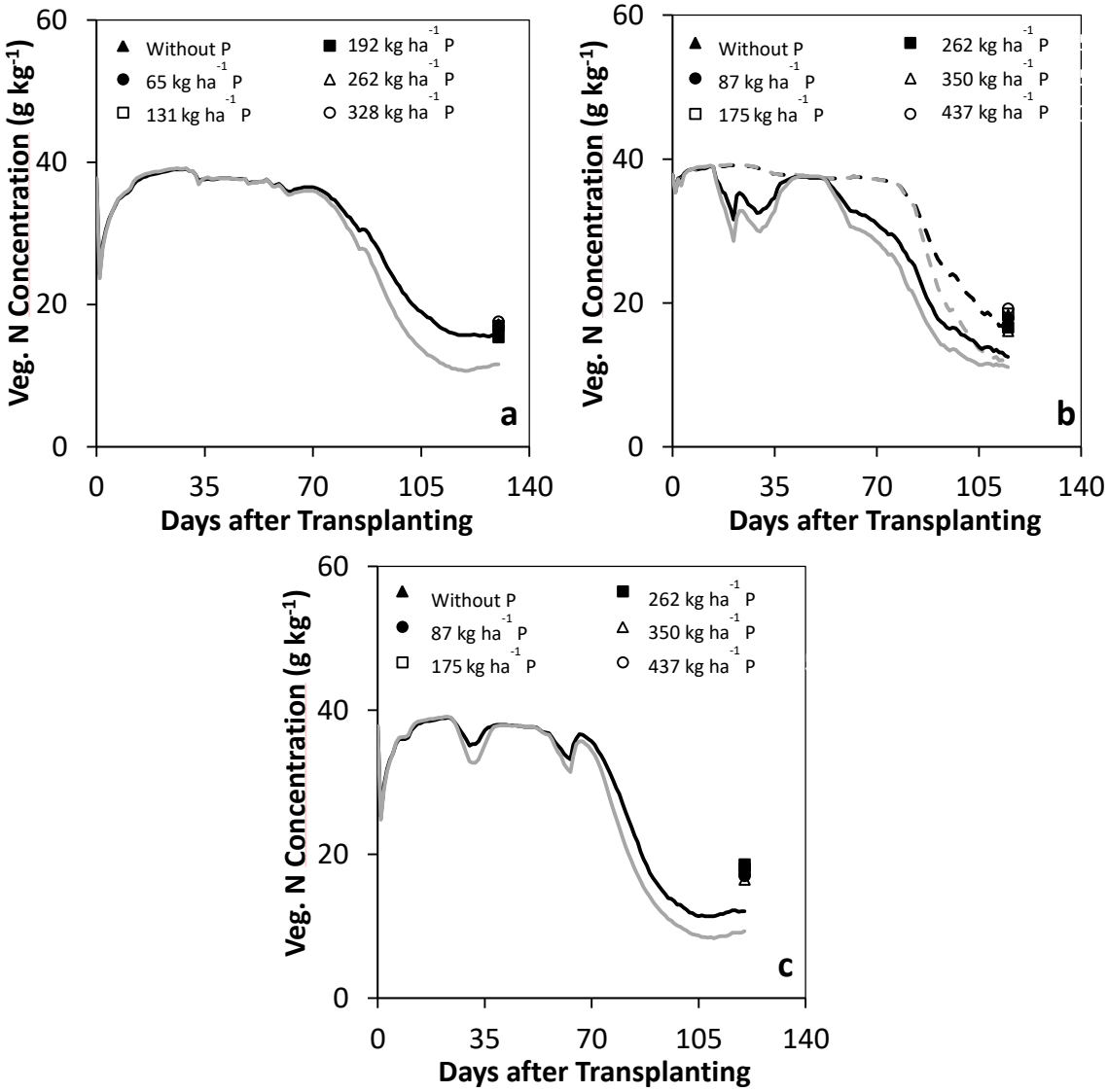

Figure 7. Observed (symbols) and simulated (lines) vegetative (leaf+stem) N concentration in tomato plants. (a) EC1 (High P); (b) EC2 (Low P); (c) EC3 (High P). Black line = Calibrated (NMOBMX, NVSMOB, SENRTE) for tomato; Gray line = The original parameterization for tomato (DSSAT V4.5). Dashed line: without P application.

At harvest, observed vegetative (leaf+stem) N concentrations were between 15 and 19 g kg^{-1}, similar to values obtained for Yan-Feng et al. (2014) of 18 to 20 g kg^{-1} at 130 DAT. The simulated N concentrations were lower (12 to 15 g kg^{-1}) than the observed, but due the calibrations of NMOBMX, NVSMOB, and SENRTE an improvement on simulation of vegetative N concentration was observed in all EC (Fig 7). The RRMSE was reduced from

0.15 to 0.09 in EC1, from 0.35 to 0.28 in EC2, and from 0.41 to 0.31 in EC3. The main factor that contributed to improve simulations of vegetative N concentration was the SENRTE calibration. By increasing SENRTE, an acceleration of senescence (loss of N-exhausted leaves per unit protein mobilized) occurs, while average N in remaining tissue appears to be stay higher because only younger leaves are left.

3.3 Plant P concentration in shoot and fruit

Simulated P optimum (critical), minimum, and actual concentration, in plant shoot and fruit, over time are shown in Figure 8. For EC1 and EC3 the model did not predicted any differences among treatments (Fig. 8a, 8b, 8e and 8f) . In both experiments, simulated P concentration in shoot was the same as the optimum concentration and even in the treatment without P fertilization. On general the model over-predicted shoot P. The simulation of P concentration in fruits for EC1 and EC3 was also similar. A peak of P concentration was observed early in the fruiting, after that, fruit P concentrations fell below P optimum until 80 DAT, then returned to P optimum until harvest. The simulations over-predicted fruit P concentration in EC1. On EC3 fruit P concentrations were over-predicted on treatments without P, 87, 175, and 262 kg ha^{-1} of P, but under-predicted on treatments 350 and 437 kg ha^{-1} of P.

Only in EC2 it was possible to see difference among treatments in the simulations of actual shoot P concentration (Fig. 8c). But after 40 DAT, the differences were smaller and shoot P concentration came close to P optimum. These results would suggest that plants in all treatments suffered different levels of P-stress throughout the season, although all simulations remained between P optimum and P minimum. The simulations of fruit P concentration did not differ among treatments, but showed fruit P concentration below P optimum in the early fruiting until 68 DAT, thereafter to the end of the season fruit P concentration remained in the

P optimum. Overall, in EC2 the model tended to over-predict shoot P concentration and fruit P concentration for treatments without P, 87, 175, and 262 kg ha^{-1} of P, and under-predicted shoot P concentration and fruit P concentration on treatments 350, and 437 kg ha^{-1} of P.

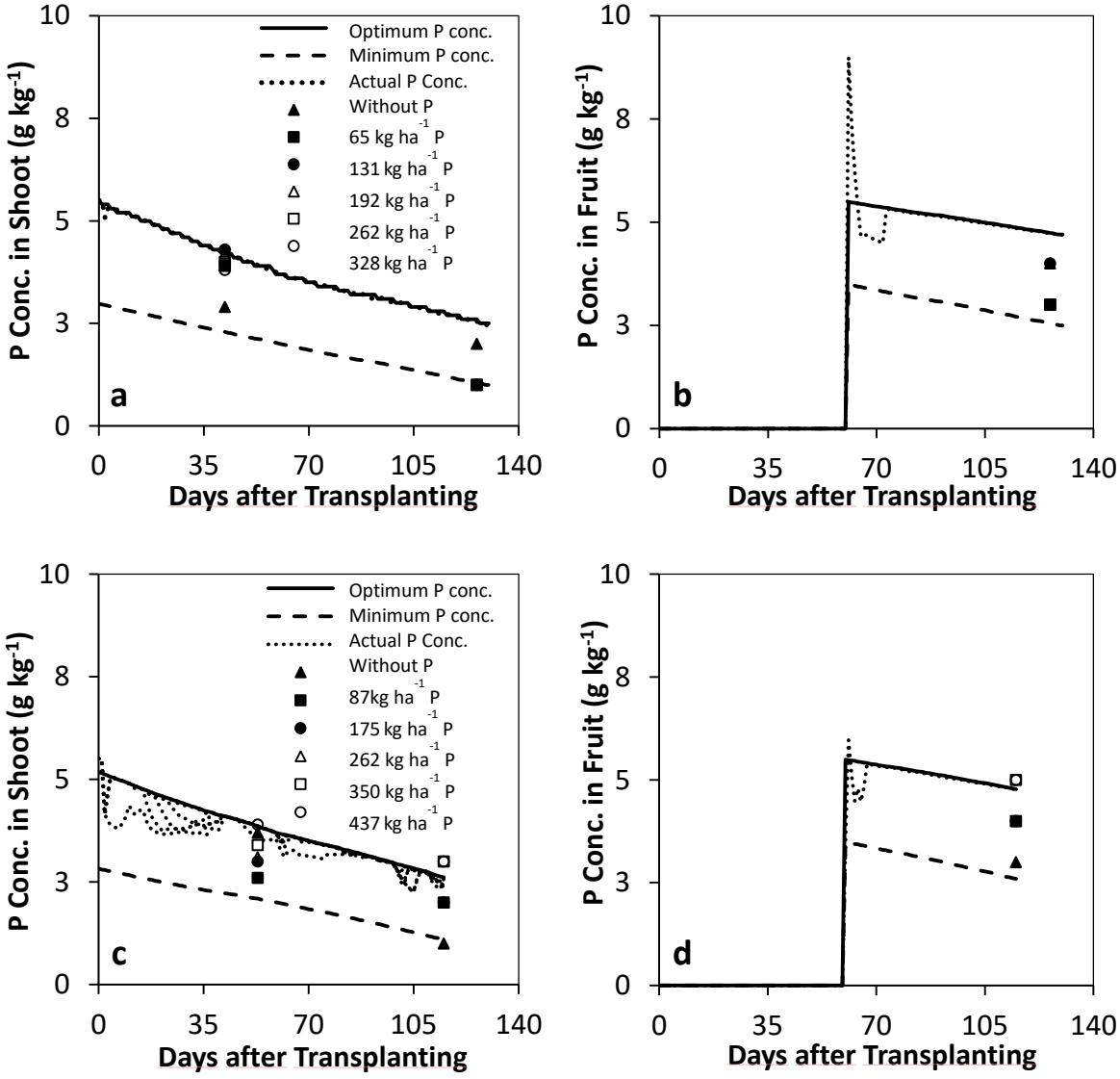

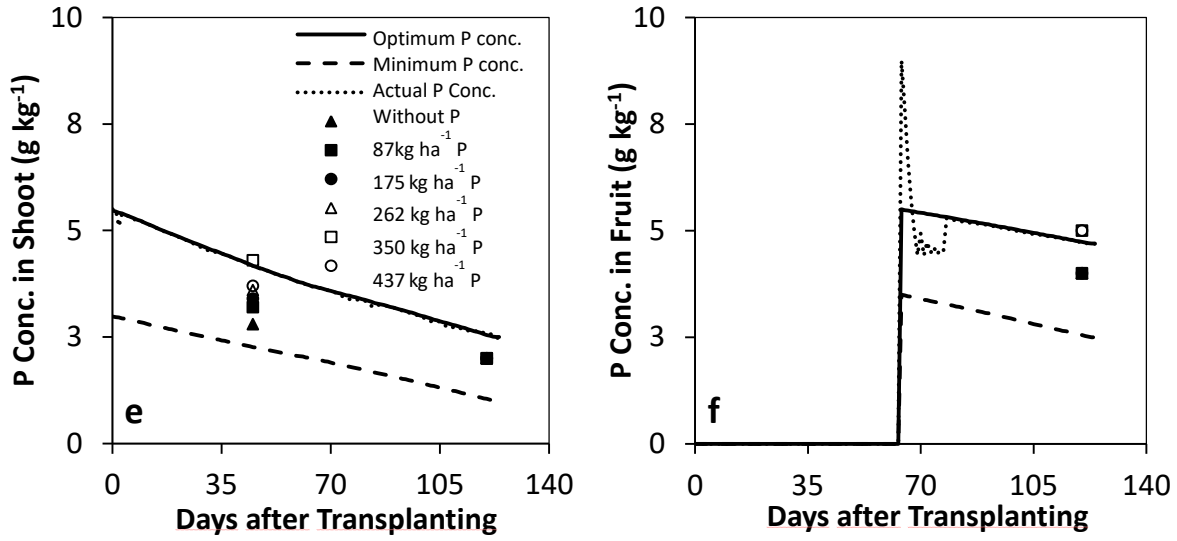

Figure 8. Observed (symbols) and simulated (lines) optimum (critical), minimum, and actual‡ P concentration in tomato plant in response to doses of P. a, b = EC1 (High P); c, d = EC2 (Low P); e, f = EC3 (High P).
‡Simulated actual P concentrations lines not seen are following the critical optimum P concentration.

The simulations of P content in shoots and fruits of ETs were comparatively accurate (Fig. 9). The tendency of the model was over-predicted P concentration in shoots. The average observed P concentration in shoots were 0.31 g kg^{-1} in ET1 and 0.28 g kg^{-1} in ET2, while the simulated value were 0.35 g kg^{-1} in ET1 and 0.34 g kg^{-1} in ET2 (Figs. 9a and 9c). The opposite was observed for simulation of P concentration in fruits of ET1(Fig. 9b) where the model tend to under-predict the average observed values of 0.51 g kg^{-1} by 18%. In spite of low accuracy of the model to simulate P concentration in fruits of ET2 (Fig. 9d) the mean simulated (0.49 g kg^{-1}) was close to the mean observed (0.47 g kg^{-1}).

In general the model weakness was to simulate initial P concentration in shoots, before 50 DAT, and in fruits, before 80 DAT. It may suggest that even though the plants and fruits are smaller (low dry matter) in initial stages of growth do not mean the P content will be concentrated.

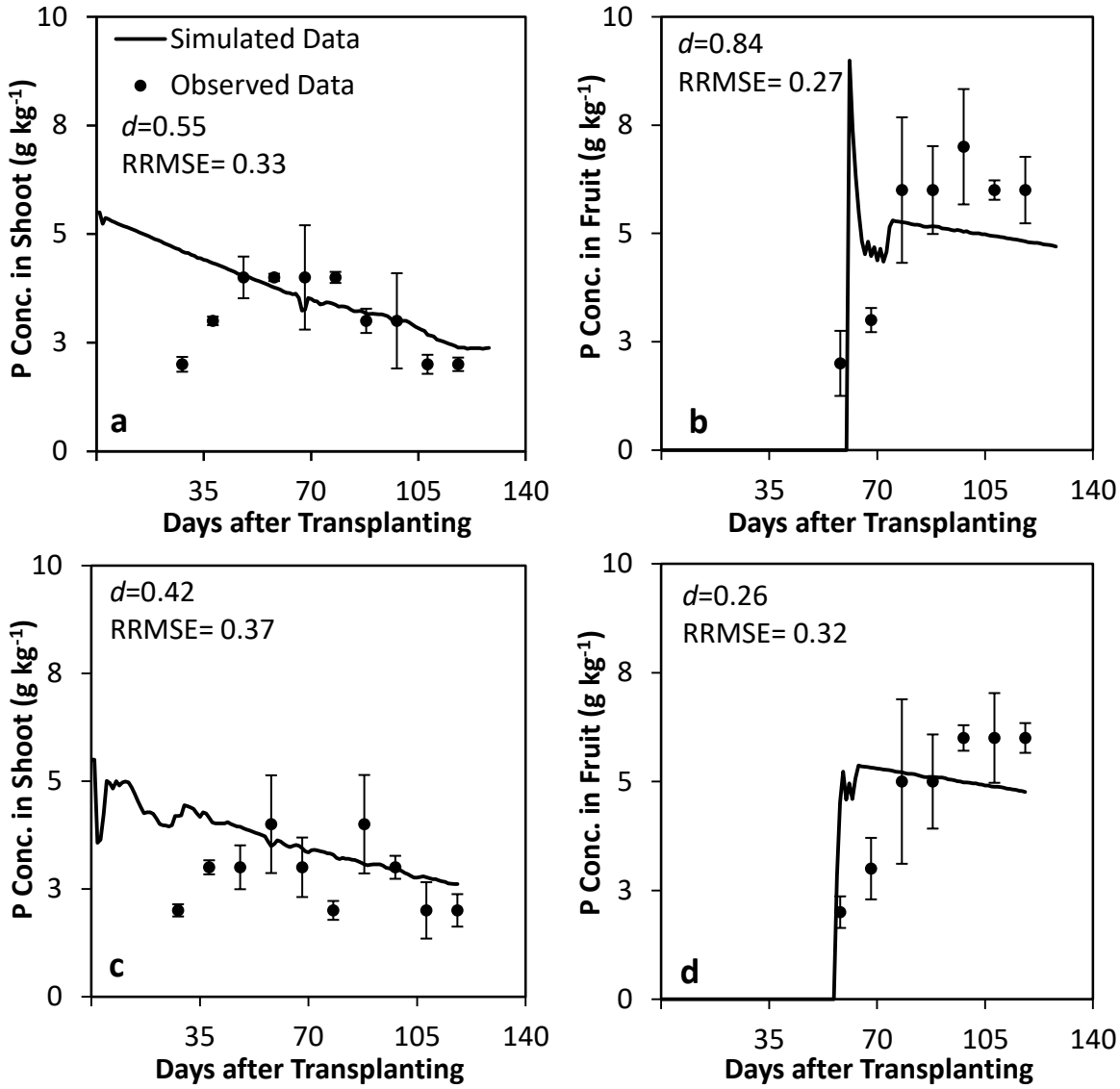

Figure 9. Observed (symbols) and simulated (lines) tomato phosphorus concentration (g kg^{-1}) in shoot (a, c) and in fruits (b, d).
a, c: Experiment for testing 1 (ET1); b, d: Experiment for testing 2 (ET2).

The model simulated difference in P concentration only when the soil had very low P content EC2 (Figs. 8c and 8d). However, in all EC and any treatment the plants did not had leaf concentration of P below that recommended by Silva and Giordano (2000) (Table 8). The capability of the model to simulate P stress can be adjusted by calibration of SRATPHOTO, the coefficient that determines shoot P concentration which values below represent reduction in photosynthesis. In this study, a value of 0.63 was used for SRATPHOTO, the same value

as calibrated by Naab et al. (2015) for peanut. Care is needed to calibrate coefficients that affect P stress since high stress sensitivity may cause reduction on biomass production.

Table 8. Observed and recommended P concentration in leaves of tomato plants.

P applied (kg ha^{-1})	EC1	EC2	EC3
	Observed P concentration (g kg^{-1})		
0	3	4	3
65	4	-	-
87	-	3	3
131	4	-	-
175	-	3	3
192	4	-	-
262	4	3	4
328	4	-	-
350	-	3	4
437	-	4	4
Recommended P concentration (Silva and Giordano, 2000)	2.5 - 7.5 (g kg^{-1})		

Conclusions

In this study, the CROPGRO-Tomato model was adapted to simulate the response of tomato plants grown in the field under tropical conditions, because no research had been done on open-field-grown (no mulch) tomato in the tropics. The model was accurate to simulate growth and yield of industrial tomato, and also had the capability of to simulate different P concentrations and reduction in yield when the soil had low P content. These results demonstrate the potential of CROPGRO-Tomato to be used under field conditions and under different P-fertilization managements. CROPGRO-Tomato model is promising to simulate tomato responses to P fertilization and the simulations can be improved by new calibrations of P concentration in plants and fruits of tomato.

References

Alvarez, V.F.C., R.R.C. Duete, T. Muraoka, W.L.C. Duete, and C.H. Abreu Jr. 2002. Soil and fertilizer phosphorus use by tomato. (In Portuguese, with English abstract). Scientia Agrícola. 59:167-172. doi: 10.1590/S0103-90162002000100024

AOAC. 1990. Official methods of analysis of the Association of Official Analytical Chemists (AOAC). AOAC, Arlington, Virginia, USA.

Besford, R.T. 1979. Uptake and distribution of phosphorus in tomato plants. Plant and soil. 51:331-340. doi: 10.1007/BF02197780

Boote, K.J., J.W. Jones, J.W. Mishoe, and G.G. Wilkerson. 1986. Modeling growth and yield of groundnut. In: M.V.K. Sivakumar, editor, Agrometeorology of groundnut. ICRISAT, Patancheru, India. p. 243-254.

Boote, K. J., J. W. Jones, and G. Hoogenboom. 1998. Simulation of crop growth: CROPGRO Model. Chapter 18. pp. 651-692. IN: R. M. Peart and R. B. Curry (eds.). Agricultural Systems Modeling and Simulation. Marcel Dekker, Inc, New York.

Boote, K.J., and J.M.S. Scholberg. 2006. Developing, parameterizing, and testing of dynamic crop growth models for horticultural crops. Acta Horticulturae. 718:23–34. doi: 10.17660/ActaHortic.2006.718.1

Boote, K.J., M.R. Rybak, J.M.S. Scholberg, and J.W. Jones. 2012. Improving the CROPGRO tomato model for predicting growth and yield response to temperature. Hortscience. 47:1038-1049.

Bryla, D. R., and R.T. Koide. 1998. Mycorrhizal response of two tomato genotypes relates to their ability to acquire and utilize phosphorus. Annals of Botany. 82:849-857. doi: 10.1006/anbo.1998.0768

Demir, K., O. Sahin, Y.K. Kadioglu, D.J. Pilbeam, and A. Gunes. 2010. Essential and non-essential element composition of tomato plants fertilized with poultry manure. Scientia Horticulturae. 127:16-22. doi:10.1016/j.scienta.2010.08.009

Jones, J.W., E. Dayan, L.H. Allen, H. Van Keulen, and H. Challa. 1989. Modeling Tomato growth for optimizing greenhouse temperatures and carbon dioxide concentrations. Acta Horticulturae. 248:285-294. doi: 10.17660/ActaHortic.1989.248.34

Kropff, M.J., S.E. Weaver, and M.A. Smits. 1992. Use of ecophysiological models for crop-weed interference: relations amongst weed density, relative time of weed emergence, relative leaf area, and yield loss. Weed Science. 40:296-301.

Lima, A.A., M.A.R. Alvarenga, L. Rodrigues, and J.G. Carvalho. 2011. Leaf nutrient content and yield of tomato grown in different substrates and doses of humic acids. (In Portuguese, with English abstract.) Horticultura Brasileira. 29:63-69. doi: 10.1590/S0102-05362011000100011

Naab, J.B., K.J. Boote, J.W. Jones, and C.H. Porter. 2015. Adapting and evaluating the CROPGRO-peanut model for response to phosphorus on a sandy-loam soil under semi-arid tropical conditions. Field Crops Research. 176:71-86. doi: 10.1016/j.fcr.2015.02.016

Parton, W.J., B. Mckeown, V. Kirchner, D.S. Ojima. 1994. CENTURY user's manual. Colorado State University, Fort Collins, CO, United States.

Porter, C.H., J.W. Jones, S.G.K. Adiku, A.J. Gijsman, O. Gargiulo, and U. Singh. 2010. DSSAT-Century soil organic matter module data requirements and initialization procedures. In: G. Hoogenboom, J.W. Jones, C.H. Porter, P.W. Wilkens, K.J. Boote, L.A. Hunt, and G.Y. Tsuji, editors. Decision Support System for Agrotechnology Transfer Version 4.5.: Overview. University of Hawaii, Honolulu, HI, United States.

Rybak, M.R. 2009. Improving a tomato growth model to predict fresh weight and size of individual fruits. Ph.D. diss., University of Florida, Gainesville, FL.

Silva, J.B.C., and L.B. Giordano. 2000. Tomato for industrial processing. Brasília: EMBRAPA Communication For Technology Transfer. 169. Embrapa-CNPH Print Office, Brasília, DC, Brazil.

Silva, E.C., and W.R. Maluf. 2012. Hydroponic technique for screening of tomato genotypes to phosphorus absorption efficiency. (In Portuguese, with English abstract.) Horticultura Brasileira. 30:317-321. doi: 10.1590/S0102-05362012000200022

Scholberg, J. 1996. Adaptive use of growth models to simulate the growth of field-grown tomato. Ph.D. diss., University of Florida, Gainesville, FL.

Singh, S., K.J. Boote, S.V. Angadi, K. Grover, S. Begna, and D. Auld. 2016. Adapting the CROPGRO model to simulate growth and yield of spring safflower in semiarid conditions. Agronomy Journal. 108:64-72. doi:10.2134/agronj15.0272

Trani, P.E., H. Nagai, and F.A. Passos. 1997. Tomato (Industrial) irrigated. In: B.Van Raij, H. Cantarella, J.A. Quaggio, and A.M.C. Furlani, editors, Technical bulletin n.100 - fertilization and liming recommendations for State of São Paulo. (In Portuguese) 2nd ed. Campinas: IAC. Campinas, SP, Brazil.

Uehara, G., and G.Y. Tsuji. 1998. Overview of IBSNAT. In: Tsuji, G.Y., G. Hoogenboom, and P.K. Thernton, editors, Understanding options for agricultural production. Springer, Netherlands. p. 1-7. doi: 10.1007/978-94-017-3624-4_1

Willmott, C.J., S.G. Ackleson, R.E. Davis, J.J. Feddema, K.M. Klink, D.R. Legates, and et al. 1985. Statistics for the evaluation and comparison of models. J. Geophys. Res. 90:8995–9005. doi:10.1029/JC090iC05p08995

Wilson, L.T., R. Tennyson, A.P. Gutierrez, and F.G. Zalom. 1987. A physiological based model for processing tomatoes: crop and pest management. Acta Horticulturae. 200:125-132. doi: 10.17660/ActaHortic.1987.200.11

Wolf, S., J. Rudich, A. Marani, and Y. Rekah. 1986. Predicting harvesting date of processing tomatoes by a simulation model. Journal American Society Horticultural Science. 111:11-16.

Yan-Feng, L., L. Jiu-Sheng, and Z. Hang. 2014. Effects of chlorination on soil chemical properties and nitrogen uptake for tomato drip irrigated with secondary sewage effluent. Journal Of Integrative Agriculture. 13:2049-2060. doi:10.1016/S2095-311

CHAPTER 3 -Methods for Estimating Leaf Area Index of Processing Tomato*

Abstract

The leaf area index (LAI) of a crop is an important parameter used on growth models. Though destructive methods continue to be used for measuring LAI, nondestructive methods are promising and affordable. Since there are no studies reporting the use of nondestructive methods for LAI estimation of processing tomato the objective of this research was to determine, with simple mathematical models, which nondestructive method, using digital images, solar radiation (Qg), sum of degree days (ΣDD) or number of leaves (NL), provide better estimations of LAI obtained by conventional (destructive) method using planimeter (leaf area meter). The study used data of LAI of processing tomato from two seasons of field production (2013 and 2014). Data were obtained using the Li-Cor leaf area meter (standard method) and two digital images methods Canopeo and ImageJ. Observed LAI was accurately estimated using image methods, NL, ΣDD, and Qg; however better results were obtained using NL (RMSE=0.2, *es*=0.7, and R^2= 0.92) and Canopeo (RMSE=0.4, *es*= 0.7, R^2= 0.93). It is possible to estimate leaf area index (LAI) of processing tomato using nondestructive methods. The estimation of LAI as a function of NL was more accurate, has the advantage of lower cost because it does not need any equipment, but it requires more time. On the other hand, the method using Canopeo also was satisfactory, has low cost, and demands less time.

*Artigo nas normas da revista Agronomy Journal

1. Introduction

Tomato is the second most produced vegetable in the world (FAOSTAT, 2013). Due the economical importance of this crop, mathematical models are often used for prediction of production in different environments or managements.

The leaf area index (LAI) of a crop is an important parameter used on crop models, it is calculated as the ratio of leaf area of canopy per unit of land area (Carvalho et al., 2011; Muller et al., 2005). LAI indicates the capability of the crop in capture light energy and thus fix CO_2 in photosynthesis, and it also influences the plant water balance via plant transpiration, therefore it is crucial for plant growth and production (Carvalho et al., 2011; Campillo et al., 2010).

Though destructive methods still are used for measuring LAI, nondestructive methods using digital images are promising and affordable (Campillo et al., 2010). There are some free software programs available for image analysis that can be used to measure LAI (Patrignani and Ochsner, 2015; Easlon and Bloom, 2014; Bylesjö et al., 2008; O'Neal et al., 2002) such as ImageJ and Canopeo (app for mobile device).

ImageJ is a public domain Java-based program for image processing. ImageJ was developed in US National Institutes of Health (NIH) in 1987, initially to be used by medical researchers, but it has become very common in many scientific fields (Schneider et al. 2012).

Canopeo is an app for analyzing images of plant canopy, available in two versions, free version for mobile devices (iOS and Android) and the complete version as a Matlab app, but the latter requires prior installation of Matlab (version R2013a or later) and Matlab image processing toolbox (8.2 or newer) (Patrignani and Ochsner, 2015).

Agrometerological models also can be used to estimate LAI as a function of solar radiation (Qg) or the sum of degree days (ΣDD). Solar radiation (Qg) has strong relationship

with LAI and the patterns of radiation intercepted and used by canopy of coffee plants (Pilau and Angeloci, 2014; Pilau and Angeloci, 2015), lemon, apple (Pereira et al., 2009), and fresh tomato (Reis et al., 2013). Also it is known that ΣDD governs changes on phenological phases of plants, and the increase or decrease of leaf area is dependent on which phenological phase the plant is in (Boote et al., 2012; Maldaner et al., 2009); therefore it is possible to estimate LAI using the ΣDD.

The generation of models to estimate LAI as a function of ΣDD is a good option because it requires no great resource, only the information of the average daily temperature and knowledge of the base temperature of the crop. In general, LAI estimations as function of ΣDD were accurate for bell peppers (Carvalho et al., 2011), maize (Muller et al. 2005) and sorghum (Narayanan et al., 2013).

Another low resource but successful method to estimate LAI is using the number of leaves per plant (NL). This method has been used to estimate LAI of some crops such as: fresh tomato (Pivetta et al., 2007), maize (Kunz et al., 2007), eggplant (Maldaner et al., 2009), and sugar cane (Streck et al., 2010), the results are quite satisfactory. However, there are no studies reporting the use of nondestructive methods for estimation of LAI of processing tomato.

Given the above, the objective of this research was to determine, from mathematical models, which nondestructive method of LAI estimation, using digital images (ImageJ and Canopeo) or as a function of solar radiation, sum of degree days, or number of leaves, provide better estimations of LAI obtained by conventional method (destructive) using the planimeter Li-Cor.

2. Materials and Methods

The experiments were carried out at two commercial tomato farms, both in Guaíra city in state of São Paulo-Brazil (20º27'S lat; 48º19'W long). The climatic classification is tropical with dry winter (Köppen = Aw; Thornthwaite = B_1rA'a'), and the annual average rainfall is 1374 mm. The soil at the experimental sites is classified as Typic Hapludox (highly weathered deep clay soil), with 52% clay, 29% silt, and 19% sand.

The transplants were established on 29 Apr. 2013 and 26 May 2014 on spacing 1.25 m x 0.25 m totaling 4 plants per m^2. The cultivar of processing tomato used in both farms was Heinz-9553, in irrigated management with application of 25 mm of water weekly, from transplanting to beginning flower, then 40 mm weekly until end of season, always discounting rainfall during the period.

After plowing and harrowing of the area, rows were opened and Urea, KCl, and Triple Super Phosphate were applied at a dose equivalent to 30 kg ha^{-1} of N, 60 kg ha^{-1} of K_2O, and 450 kg ha^{-1} of P_2O_5, respectively, then mechanized transplanting of seedlings was done and the rows were closed. At 30 and 50 days after transplanting (DAT) 60 kg ha^{-1} of N was applied. Also 160 kg ha^{-1} of K_2O was applied in three split applications at 45, 65 and 85 DAT.

Every 15 d during crop cycle (about 120 d) 24 plants were taken randomly for leaf area index (LAI) determination using Li-Cor (LI-3100C Area Meter) standard method. Also for determination of LAI using the digital images methods, ImageJ 1.48v (Rasband, 1997) and Canopeo (version for mobile device) (Patrignani and Ochsner, 2015), a square frame of $1m^2$ was placed on the floor above the plant canopy, and 24 pictures were taken on high of approximately 1.40m, right above the plant canopy, using a photographic camera SONY Cyber-shot (14.1 mega pixels) (Fig. 1A).

For determination of LAI all green leaves (leaflets and petioles) of each plant were separately passed through the Li-Cor leaf area meter. At this time it was counted the number of leaves (NL) per plant.

To measure LAI using ImageJ, it is necessary to have a reference of distance to set the scale, in this experiment it was used the square frame of $1m^2$, then the image was converted into 8 bit. Next steps are the calibration of threshold and conversion of the image in binary, thus the area is measured according to the used scale (Table 1; Fig. 1).

Table 1. Steps for measuring leaf area using ImageJ program.

Steps	Commands	Action	Image type
1	File/Open/Straight	Use the *Straight* tool to draw a line with known scale/OK (Figure 1. A)	JPEG
2	Analyze/Set Scale	Set: Known Distance and Unit of Length	JPEG
3	Image/Type	Set: 8-bit (Figure 1. B)	8-bit
4	Image/Adjust/Threshold	Calibrate threshold/Apply	8-bit
5	Process/Binary	Hit: Make Binary (Figure 1. C)	Binary
6	Polygon	Use the *Polygon* tool to cut the picture if necessary (Figure 1. D)	Binary
7	Analyze/Analyze Particles	Set: Show Masks, Display results, and Summarize/OK	Binary
8	Summary	See: Total Area	Binary

In Canopeo, before processing the images, the pictures were cut to keep $1m^2$ of area, then the images were downloaded from phone gallery and automatically converted by the app to binary (Fig. 1 A, E, and F). The leaf area is given in percentage of total area of the picture. To convert to LAI the values were divided by 100.

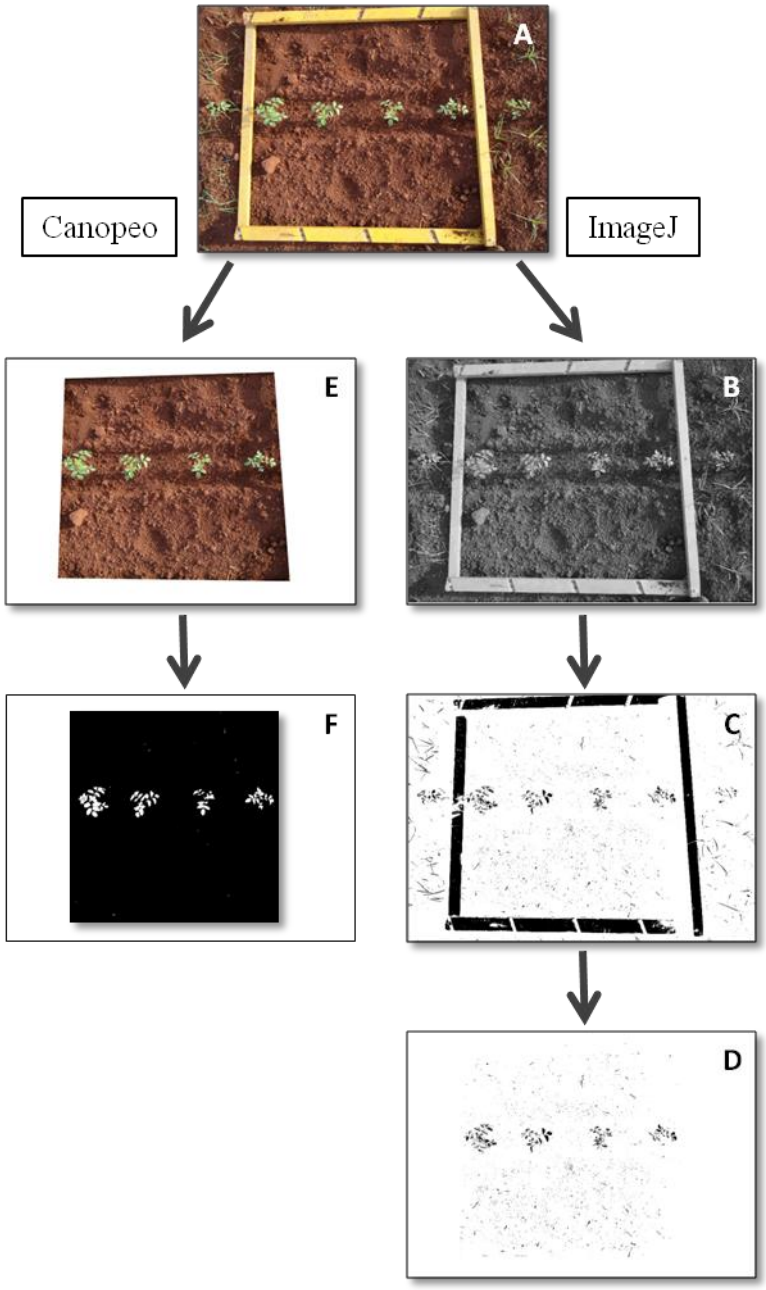

Figure 1: Image of tomato canopy (15 d old) being processed in ImageJ (A, B, C, and D) and Canopeo (A, E, and F).

The data obtained using Li-Cor were used for estimation of LAI as a function of ImageJ and Canopeo using a potential equation. To estimate LAI as a function of NL it was used a linear equation. LAI also was estimated as a function of sum of degree days (ΣDD) and

global radiation (Qg) using a log-normal model [1]. The same model was used to estimate NL as a function of ΣDD and Qg.

$$Y = Yo + \frac{A}{wX\sqrt{2\pi}} e^{\frac{-[\ln X/xc]^2}{(2w)^2}} \quad [1]$$

Where: *Y* = LAI or NL; *X* = Qg or ΣDD; *Yo* = the initial value of *Y*; *xc* = the central value of *X*; *w* = the curvature coefficient, and *A* = amplitude factor.

The *w* coefficient affects jointly the *Y* peak and the time (ΣDD) of occurrence (Figure 2A), while *A* factor determines the amplitude value of *Y* (Figure 2B). Both parameters are related to genetic coefficients and may be different depending on the tomato cultivar. The parameters *Yo*, *xc*, *w* and *A* were calibrated using the mathematical method GRG2-Generalized Reduced Gradient (Lasdon and Waren, 1978) with the objective to minimize the sum of squared errors. This method is wide used in non-linear problems due it robustness.

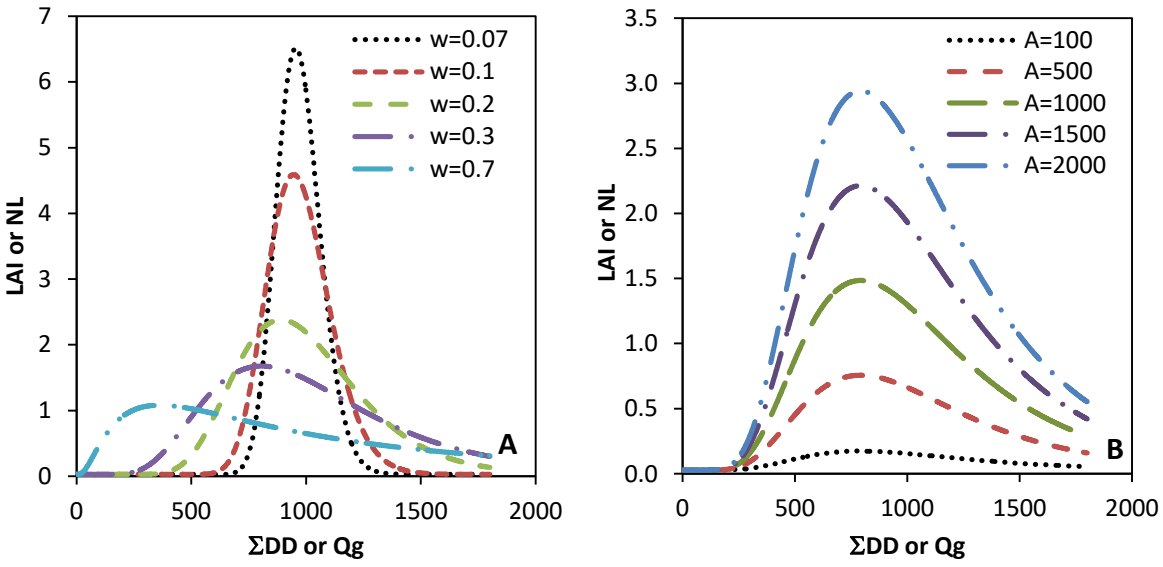

Figure 2: Shape of curves when varying *w* (curvature adjustment coefficient)(A), and varying *A* (amplitude factor) (B).

The weather data of maximum and minimum air temperature (ºC), rainfall (mm), wind speed (*u*) (m s^{-1}), global radiation (Qg) (W m^{-2}), and relative humidity (RH) (%) were daily

measured by an Automatic Weather Station located at the experimental sites. To obtain the ΣDD the following equation was used:

$$\sum DD = \sum(\overline{T}_d - t) \quad [2]$$

Where: $\overline{T}_d$ is the average daily temperature and *t* is the base temperature of the crop (for tomato = 10°C).

The models were evaluated in terms of accuracy by the root mean square error (RMSE) [3], precision by the coefficient of determination (R^2) [4], and tendency by systematic error (*se*) [5].

$$\text{RMSE} = \sqrt{\sum_{i=1}^{N} \frac{(Yobs_i - Yest_i)^2}{N}} \quad [3]$$

Where: *N* is the number of observations, $Yobs_i$ is the observed value for *i*th measurement, $Yest_i$ is the estimated value for the *i*th measurement. The RMSE is always positive and the closer to zero the better is the agreement between observed and estimated data.

$$R^2 = \frac{\sum_{i=1}^{N}(Yest_i - \bar{Y})^2}{\sum_{i=1}^{N}(Yobs_i - \bar{Y})^2} \quad [4]$$

Where: *N* is the number of observations, $Yobs_i$ is the observed value for *i*th measurement, $Yest_i$ is the estimated value for the *i*th measurement, $\bar{Y}$ is the average of the estimated value for the *i*th measurement.

$$se = \sqrt{\sum_{i=1}^{N} \frac{(Yobs_i - \bar{Y})^2}{N}} \quad [5]$$

Where: *N* is the number of observations, $Yobs_i$ is the observed value for *i*th measurement, $\bar{Y}$ is the average of the estimated value for the *i*th measurement.

3. Results and Discussion

The weather characteristics during evaluation of LAI in both years are presented on Figure 3. Although both experiments were irrigated, the RH in 2013 was higher, with average of 39%, due to the higher cumulated rainfall (171 mm), while in 2014 average RH was 30%

and rainfall was 64 mm. These were the main difference in weather between the years of evaluation, while Tmax, Tmin, *u*, and Qg were similar in both years, with average of 29°C, 13.5°C, 2.2 m s^{-1}, and 16.3 W m^{-2}, respectively.

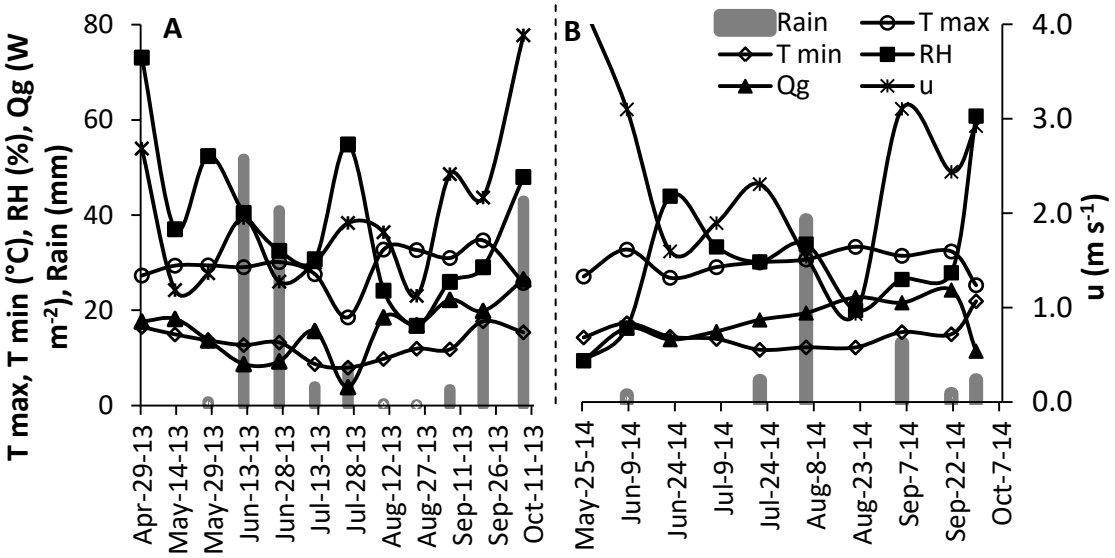

Figure 3: Weather data at experimental sites during growing season. (A) Experiment 1; (B) Experiment 2. Tmax= Maximum temperature; Tmin= Minimum temperature; RH= relative humidity; Qg= global radiation; and rain. Biweekly average.

The values found for leaf area index observed (LAI_{obs}) using Li-Cor were higher than when using digital images (Fig. 4 A). It may occur because of all leaves were used to measure LAI_{obs} using Li-Cor, whereas images are, presumably, measuring just of leaves seen in images rather than leaves covered up by higher exposed leaves. The highest LAI_{obs} obtained by Li-Cor was 1.8 m^2 m^{-2} at 75 DAT, smaller to those values found by Reis et al., (2013) of 2.78 at 70 DAT for fresh tomato. It is important to remember that fresh tomato has indeterminate growth habit and leaf production is continuous for a long period until apical pruning. The processing tomato has determinate growth habit and it grows in contact with the soil. These factors contribute to the loss of leaves, therefore LAI tends to be smaller.

Since the area of $1m^2$ was fixed for the methods using the digital images, LAI_{obs} would never be higher than $1m^2m^2$ because these methods only pick up the leaves on surface (under

radiation), therefore the overlap of leaves can be one source of error for LAI estimations when using digital images, nonetheless Canopeo was able to detected a great portion of shaded leaves of maize (Patrignani and Ochsner, 2015).

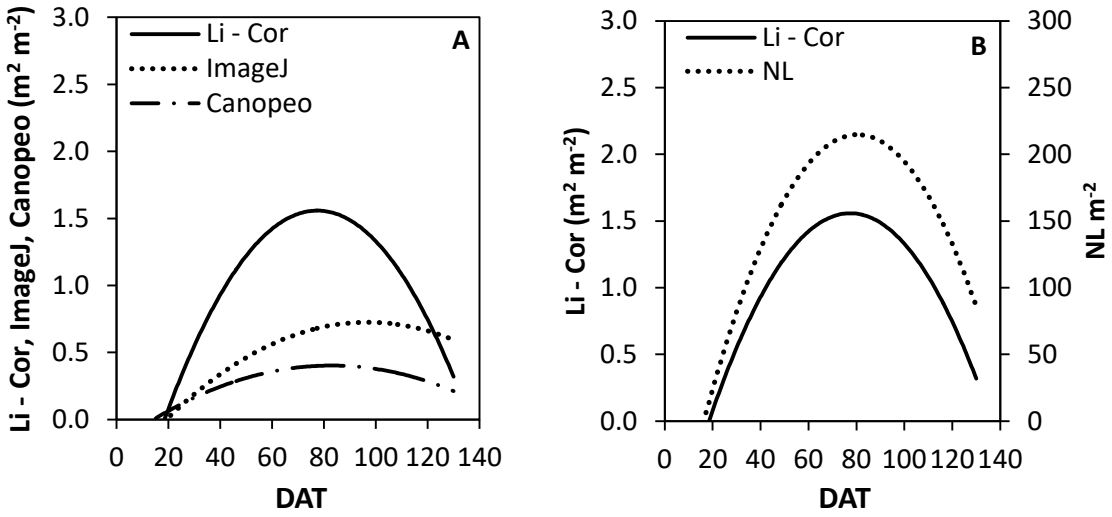

Figure 4: Observed leaf area index (LAI_{obs}) determined by Li-Cor, ImageJ, and Canopeo (A). LAI_{obs} determined by Li-Cor and number of leaves (NL m^{-2}) (B). DAT= Days after transplant.

Comparing LAI_{obs} using ImageJ and Canopeo it is possible to note higher values using ImageJ. The characteristics of the methods are the cause for this difference. When the image is converted to binary (black and white) the process in ImageJ assumes that all objects on image are black and the background is white (Ferreira and Rasband, 2012). In this case the area of other material on surface, not only leaves, could be counted as leaf area. Canopeo, however, converts to white the pixels that satisfy the criteria of green canopy, and converts to black the pixels that did not satisfies this criteria, therefore undesired pixels rarely will be selected as leaf area and the overestimation is reduced (Patrignani and Ochsner, 2015) (Fig. 1 F).

Number of leaves (NL) increases until fruiting and then decreases to the harvest date, proportionally to leaf area (Fig. 4 B), therefore NL can be used to estimate LAI. Increasing

and decreasing leaf area is an important characteristic of processing tomato with determinate growth habit. Researchers have shown that the weakness of some models is not to reproduce properly the leaf area decreases occurring near the end of season (Boote et al., 2012). This problem is minimized when using NL to estimate LAI.

The estimation of LAI_{est} *f* (ΣDD) using a log-normal model (Fig.5 A) was fairly accurate (RMSE= 0.4; R^2=0.68; *se* = 0.7). Reis et al, (2013) found high agreement (R^2= 0,97) for estimating LAI as a function of DAT of fresh tomato in an experiment conducted in greenhouse. Although DAT has close relation with ΣDD and good correlation with LAI, the number of calendar days for a crop to complete its cycle is variable. However, it is known that the changes in phenological phases of a crop are dependent on the accumulated degree days and LAI will increase or decrease depending on which developmental phase the plant is in (Boote et al., 2012).

Müller et al. (2005) used a segmented linear model to estimate LAI of maize as a function of ΣDD where each segment corresponds to a developmental phase of the crop, and obtained good agreement between observed and estimated data (R^2= 0,97). Also for bell pepper Carvalho et al. (2011) divided the crop cycle into three phenological phases (I - initial growth; II - maximum vegetative growth; III - production) and achieved good fit with exponential model for phase I (R^2 = 96.2) and linear models for phases II (R^2 = 91.5) and III (R^2 = 74.4) in function of ΣDD.

The estimation of LAI_{est} *f* (Qg) using the log-normal model was also fairly accurated (RMSE= 0.7; R^2=0.64; *se* = 0.4) (Fig. 4 B). However, Pilau and Angelocci (2014) obtained good estimation of net radiation per unit of leaf area of coffee as a function of Qg (average R^2= 0.89). These results demonstrate that Qg would be more correlated to efficiency of use of

radiation by plant canopy than with LAI itself. Also it was reported the specific leaf area depends on the interaction between Qg and temperature (Boote et al., 2012).

Leaf area index simulations using log-normal model as a function of ΣDD and Qg reproduced properly the reduction in LAI which occurs late on the season due senescence, N-mobilization, and the growth habit of processing tomato, contrary to what was reported by Boote et al. (2012) for some crop models. That is an advantage of using the this model to estimate LAI of processing tomato.

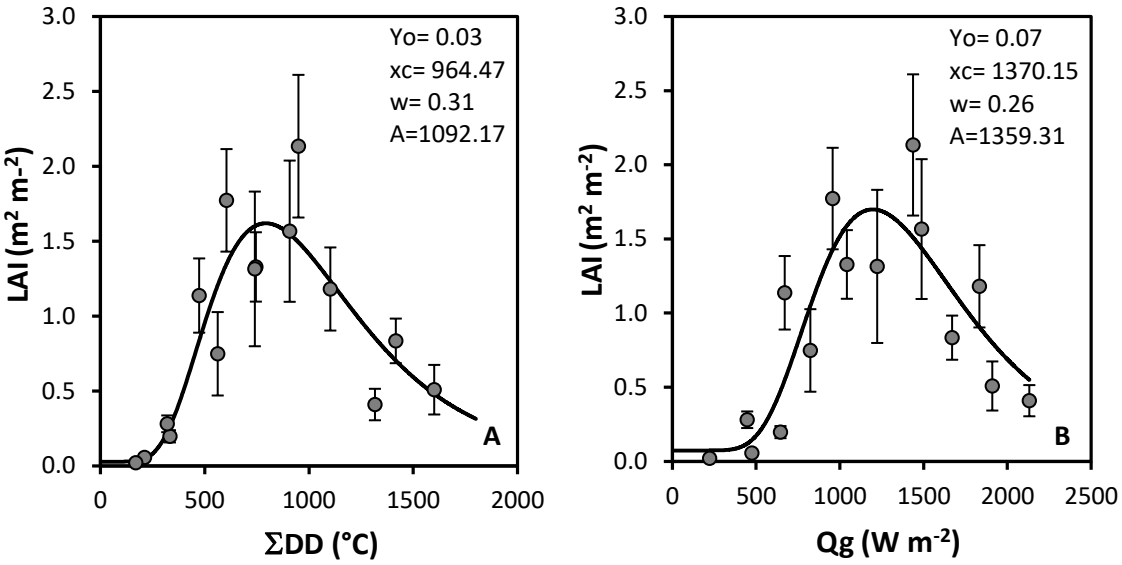

Figure 5: Estimation of leaf area index (LAI) of processing tomato as a function of ΣDD (A) and as a function of (Qg) (B). Symbols= Observed LAI; Lines= Estimated LAI.

The maximum rate of increasing LAI obtained by the log-normal model was 0,004 m^2 m^{-2} at 457 ºC cumulated degree days and maximum LAI (1.61 m^2 m^{-2}) was observed at 769 ºC cumulated degree days. For LAI estimation using Qg, maximum rate of increasing LAI was 0.007 m^2 m^{-2} observed at 770 W m^{-2} accumulated and the higher value was 1.7 m^2 m^{-2} at 1,196 W m^{-2} accumulated.

Number of leaves was a very good parameter for LAI estimation of processing tomato. The estimation of LAI_{est} *f*(NL) using linear model was accurate (RMSE=0.2, *es*=0.7, and R^2=

0.92) (Fig. 6 A), on average the area per leaf was 74 cm^2. Pivetta et al. (2007) obtained high precision for estimation of LAI as a function of number of leaves of fresh tomato with undetermined growth habit (R^2=0.86) and determined growth habit (R^2=0.94), however using exponential model.

Good estimation of leaf area as a function of number of leaves also was reported for sugar cane (R^2> 0.88) using the Gompertz equation (Sinclair et al., 2004). The results of these studies indicate an attractive alternative for LAI estimation using NL, since this method has the advantage of being easy, nondestructive, and has no cost compared with methods which require equipment.

In case it is not possible to count the NL on the field, there are the alternative to estimate NL_{est} *f*(ΣDD) (RMSE= 44, *es*=83, and R^2= 0.99) and NL_{est} *f*(Qg) (RMSE= 40, *es*=83 and R^2= 0.77) using a log-normal model (Fig. 6 B and C) with accurate adjustment. The thermal sum was reported as main ecological factor that determines the appearance of leaves in tomato (Pivetta et al., 2007), eggplant (Maldaner et al., 2009), and sorghum (Narayanan et al., 2013). Pivetta et al. (2007) reported the estimation of NL as a function of ΣDD had linear adjustment for three genotypes of tomato with different leaf sizes, and obtained high coefficients of determination (R^2> 0.92). Linear regressions also resulted in $R^2 \geq 0.86$ for estimation of NL as a function of ΣDD of four cultivars of sugar cane (Sinclair et al., 2004).

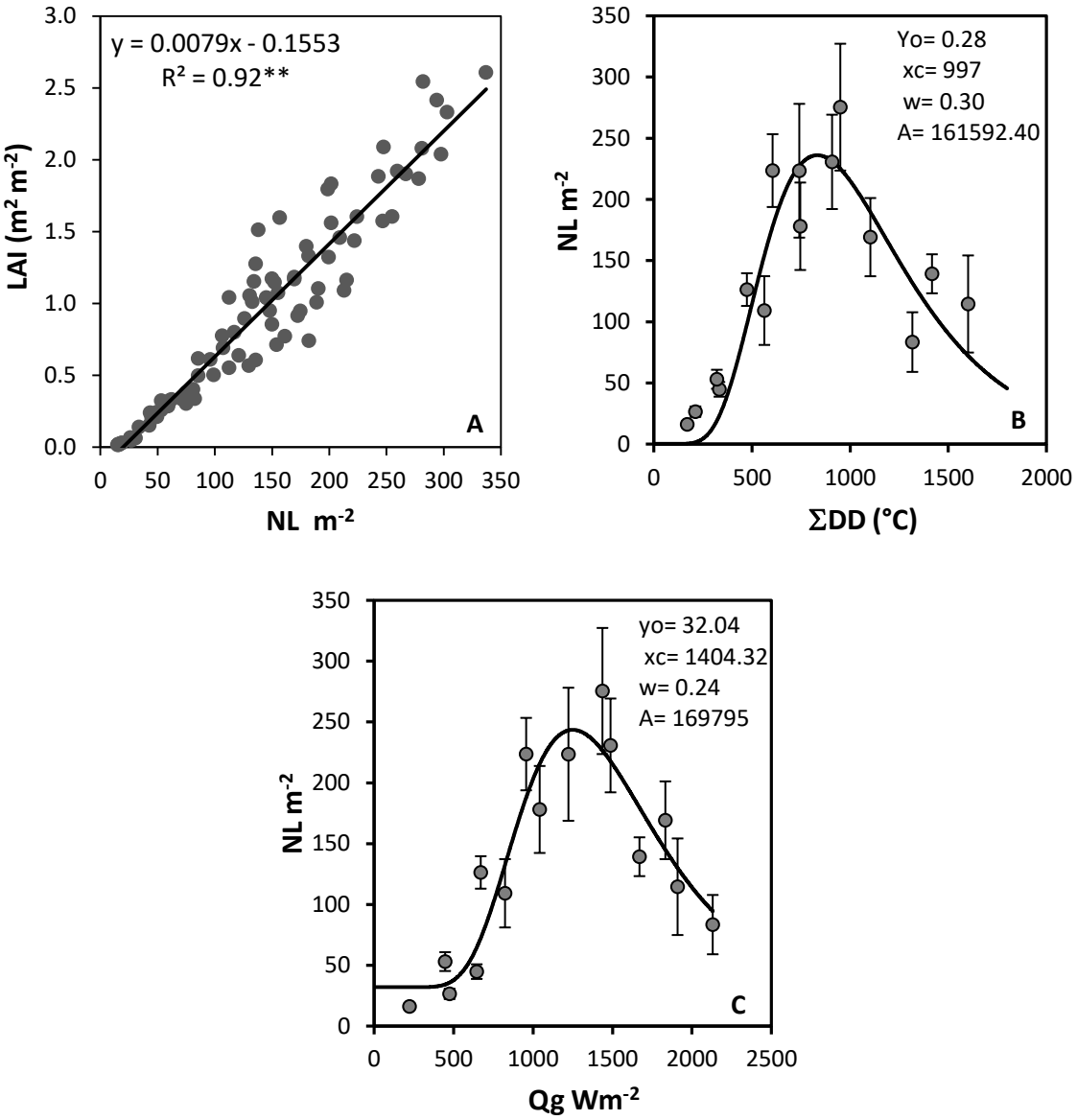

Figure 6: (A) Estimation of leaf area index (LAI_{est}) as a function of NL. (B) Estimation of NL as a function of ΣDD. (C) Estimation of NL as a function of Qg.
NL= number of leaves; Symbols= observed NL; Lines = estimated NL.

The use of digital images to estimate LAI is a nondestructive alternative. Canopeo method provided better estimation LAI_{est} (RMSE=0.4, *es*= 0.7, R^2= 0.93) than ImageJ method (RMSE=0.5, *es*= 0.7, R^2= 0.75) using potential equation (Fig. 7). Possibly Canopeo had better performance because it was used with automatic calibration while ImageJ, in this study, was manually calibrated.

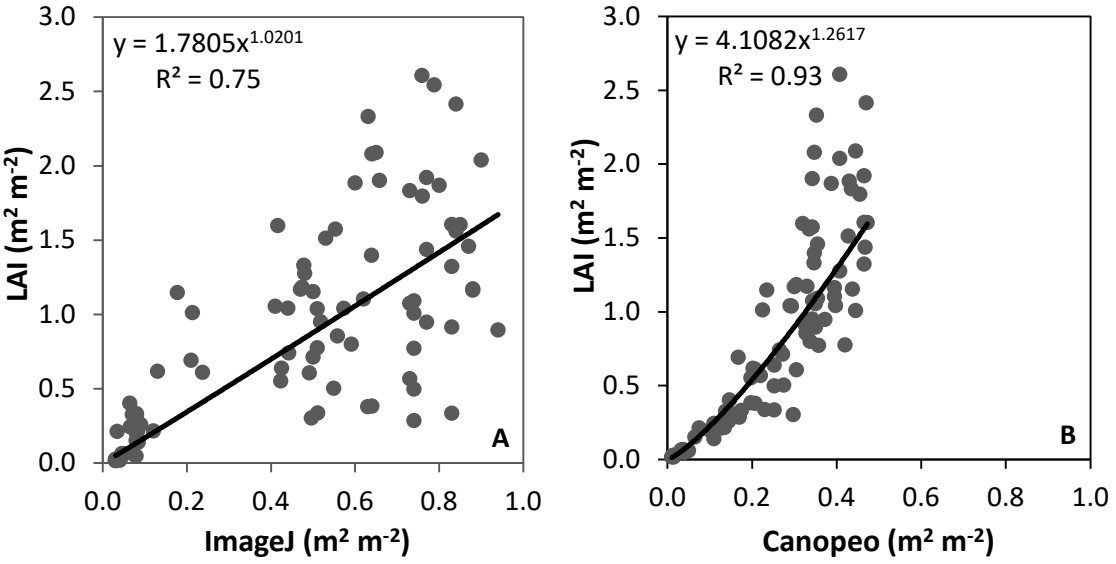

Figure 7: Estimation of leaf area index LAI_{est} as a function of ImageJ (A), and Canopeo (B). Symbols= observed LAI ; Lines = estimated LAI.

The manually calibration of ImageJ could be the reason of more variability on the data obtained using this method (Fig. 7A). On the other hand, a linear regression described accurately (R^2 = 0.99) the relationship between Li-Cor and ImageJ on measurements of leaf area of soybean (O'Neal et al., 2002).

Patrignani and Ochsner (2015) compared Canopeo with two other softwares for image analyzing, SamplePoint 1.56 (manual pixel classification) and Sigma Scan Pro 5 (automatic color threshold) to determine fractional green canopy cover of maize, forage sorghum, turf, and switchgrass, and obtained very good agreement between the methods (average RMSE=0.068). Also a high correlation (R^2 = 0.99) was found when comparing the method ImageJ against to software LAMINA (Leaf shApe deterMINAtion) for leaf area determination of *Artemisia annua* (Bylesjö et al., 2008).

The methods using digital images are, basically, the same as fraction light interception that is directly related with photosynthetically active radiation (PAR) according to Monsi-

Saeki theory (Monsi and Saeki, 2005; Hirose, 2005) and can be a valuable method for LAI estimation and utilization in photosynthesis models.

The variability in NL and leaf area of processing tomato (determinant growth) makes it difficult to simulate LAI. This variability occurs especially from the middle of crop life cycle. The rapid loss of leaves that occurs close to the harvest in many crops depends on environmental characteristics (Streck et al., 2006; Streck and Aberto, 2006), and it is accentuated for processing tomato because the plants grow in contact with soil. Also the decline of LAI near to harvest can be associated with senescence and N remobilization (Boote et al., 2012).

Loss of leaves does not occur in early stages of the culture, as long as there is no external interference, therefore LAI is better simulated during that time by different methods, however, throughout the crop cycle, LAI_{est} using NL was the closest to LAI_{obs} (Fig. 8).

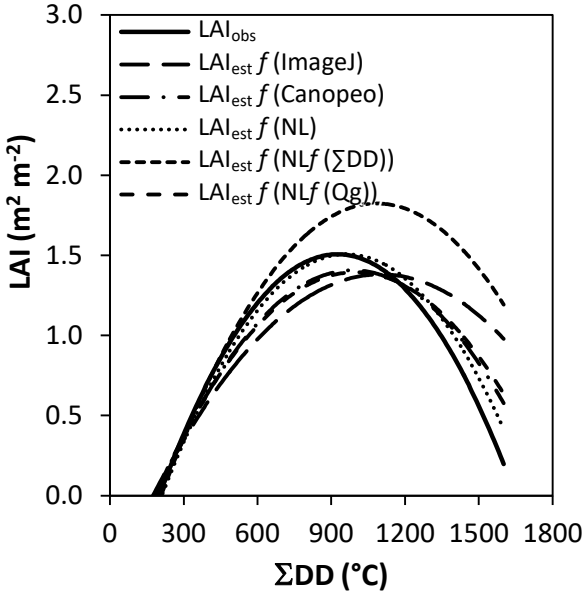

Figure 8: Observed leaf area index (LAI_{obs}) and estimated LAI(LAI_{est}) as a function of different methods. ΣDD = Sum of degree days.

Conclusions

It is possible to estimate leaf area index (LAI) of processing tomato using non-destructive methods of number of leaves (NL) and digital images, also using the sum of degree days and solar radiation. The estimation of LAI as a function of NL was accurate, has the advantage of to be low cost because does not need any equipment, but requires more time on field compared to image methods.

Estimation of LAI as a function of Canopeo was accurated, has low cost, and demands less time. Possibly LAI estimation using Canopeo would be improved if using the complete version with Matlab (paid). Also estimation of LAI as a function of ImageJ should be tested using automatic calibration of the method to pursue better results.

Estimation of LAI as a function of the sum of degree days and solar radiation is a promising alternative that do not need to be on field and should be further explored.

References

Bylesjö, M., Segura, V., Soolanayakanahally, R. Y., Rae, A. M., Trygg, J., Gustafsson, P., Jansson, S & Street, N. R. (2008). LAMINA: a tool for rapid quantification of leaf size and shape parameters. BMC Plant Biology, 8(1), 82.

Boote, K.J., M.R. Rybak, J.M.S. Scholberg, and J.W. Jones. 2012. Improving the CROPGRO tomato model for predicting growth and yield response to temperature. Hortscience. 47:1038-1049.

Campillo, C., Garcia, M. I., Daza, C., & Prieto, M. H. (2010). Study of a non-destructive method for estimating the leaf area index in vegetable crops using digital images. HortScience, 45(10), 1459-1463.

Carvalho, D. F., de Oliveira, A. D., & Pereira, J. B. A. (2011). Model adjustment for estimating bell pepper leaf area index and dry mass accumulation as a function of degree days. Semina: Ciências Agrárias (Londrina), 32(3), 971-982.

Easlon, H. M., & Bloom, A. J. (2014). Easy Leaf Area: Automated digital image analysis for rapid and accurate measurement of leaf area. Applications in plant sciences, 2(7).

FAOSTAT (2013) – Food and Agriculture Organization of The United Nations Statistics. Top 50 Commodities. <http://faostat3.fao.org/browse/rankings/commodities_by_regions/E> Access:08/16/2016.

Ferreira, T.; Rasband, W. (2012). ImageJ user guide. IJ1. 46r. Natl. Inst. Health, Bethesda, MD. <https://imagej.nih.gov/ij/docs/index.html>. pdf.

Hirose, T. (2005). Development of the Monsi–Saeki theory on canopy structure and function. Annals of Botany, 95(3), 483-494.

Lasdon, L. S. and Waren, A. D. (1978). GRG 2 user's guide. Cleveland, Ohio.

Kunz, J. H., Bergonci, J. I., Bergamaschi, H., Dalmago, G. A., Heckler, B. M. M., & Comiran, F. (2007). Uso da radiação solar pelo milho sob diferentes preparos do solo, espaçamento e disponibilidade hídrica. Pesquisa agropecuaria brasileira: 1977. Vol. 42, n. 11,p. 1511-1520.

Maldaner, I. C., Guse, F. I., Streck, N. A., & Heldwein, A. B., Lucas, D. D. P., Loose, L. H. (2009). Filocrono, área foliar e produtividade de frutos de berinjela conduzidas com uma e duas hastes por planta em estufa plástica. Ciência Rural, 39(3).

Monsi, M. and Saeki, T. (2005). On the factor light in plant communities and its importance for matter production. Annals of Botany, 95(3), 549-567.

Müller, A. G., Bergamaschi, H., Bergonci, J. I., Radin, B., França, S., & Silva, M. I. G. (2005). Estimativa do índice de área foliar do milho a partir da soma de graus-dia. Revista Brasileira de Agrometeorologia, 13(1), 65-71.

Narayanan, S., Aiken, R. M., Prasad, P. V., Xin, Z., Paul, G., & Yu, J. (2014). A simple quantitative model to predict leaf area index in sorghum. Agronomy Journal, 106(1), 219-226.

O'Neal, M. E., Landis, D. A., & Isaacs, R. (2002). An inexpensive, accurate method for measuring leaf area and defoliation through digital image analysis. Journal of Economic Entomology, 95(6), 1190-1194.

Patrignani, A., & Ochsner, T. E. (2015). Canopeo: A Powerful New Tool for Measuring Fractional Green Canopy Cover. Agronomy Journal, 107(6), 2312-2320.

Pereira, A. B., Nova, N. V., & Alfaro, A. T. (2009). Necessidades hídricas de citros e macieiras a partir da área foliar e da energia solar. Revista Brasileira de Fruticultura, 31, 671-679.

Pilau, F. G., & Angelocci, L. R. (2014). Balanço de radiação de copas de cafeeiros em renques e suas relações com radiação solar global e saldo de radiação de gramado. Bragantia, Campinas, 73(3), 1-10.

Pilau, F. G., & Angelocci, L. R. (2016). Padrões de interceptação de radiação solar por cafeeiros em função da área foliar. Coffee Science, 11(1), 127-136.

Pivetta, C. R.; Tazzo, I. F., Maass, G. F., Streck, N. A., & Heldwein, A. B. (2007). Emissão e expansão foliar em três genótipos de tomateiro (*Lycopersicon esculentum* Mill.). Ciência Rural, 37(5).

Rasband, W.S. (1997). ImageJ. U. S. National Institutes of Health, Bethesda, Maryland, USA, http://imagej.nih.gov/ij/.

Reis, L. S., de Azevedo, C. A., Albuquerque, A. W., & Junior, J. F. (2013). Índice de área foliar e produtividade do tomate sob condições de ambiente protegido. Revista Brasileira de Engenharia Agrícola e Ambiental, 386-391.

Schneider, C. A., W. S. Rasband, and K. W. Eliceiri. 2012. NIH Image to ImageJ: 25 years of image analysis. Nature Methods 9: 671 – 675 .

Sinclair, T. R., Gilbert, R. A., Perdomo, R. E., Shine, J. M., Powell, G., & Montes, G. (2004). Sugarcane leaf area development under field conditions in Florida, USA. Field Crops Research, 88(2), 171-178.

Streck, N. A., Hanauer, J. G., Gabriel, L. F., Buske, T. C., & Langner, J. A. (2010). Leaf development and growth of selected sugarcane clones in a subtropical environment. Pesquisa Agropecuária Brasileira, 45(10), 1049-1057.

Streck, N. A., Lago, I., Alberto, C. M., & Bisognin, D. A. (2006). Simulação do desenvolvimento da batata cultivar Asterix em cinco cenários de mudanças climáticas em Santa Maria, RS. Bragantia, 65(4), 693-702.

Streck, N. A., & Alberto, C. M. (2006). Estudo numérico do impacto da mudança climática sobre o rendimento de trigo, soja e milho. Pesquisa Agropecuária Brasileira, 41(9), 1351-1359.

CHAPTER 4 - Accumulation of biomass and nutrients by processing tomato*

Abstract - Brazil is the seventh largest producer of processing tomato, therefore the factors related to plant nutrition and production are relevant in the scientific community. The objective of this study was to characterize the accumulation of biomass and nutrients by processing tomatoes grown in high and low fertility soils. Two experiments were conducted in 2013, one in high fertility soil (HF) and the other in low fertility soil (LF), to quantify the biomass and nutrient accumulation by plants samples were collected every ten days (30 to 120 days after transplanting) at random, with four replications (three plants per replications). The collected plants were divided into vegetative parts (stems + leaves = VB) and fruits (FR) then dried at 65 ° C. The dried material was used to determine biomass and nutrients accumulated in VB and FR, separately. Accumulations of biomass in VB and FR of processing tomato, grown in HF and LF soil were adjusted to the quadratic model. The descending order of nutrient accumulation by tomato was K, N, Ca, P, Mg, S, Fe, Cu, Mn, Zn in HF soil, and K, N, Ca, P, Mg, S, Fe, Mn, Cu, Zn in LF soil. Tomato plants grown in HF and LF soils, however with same fertilization, have similar potential of biomass production.

Keywords: *Solanum lycopersicum***,** Plant physiology, Nutrient uptake, Plant nutrition

Introduction

The processing tomato is a vegetable of great economic importance for Brazil, and it is cultivated mainly in the Mid-West and Southeast regions. Brazilian production of processing tomato may have reached 1.4 million tons in 2015, this production kept Brazil as the eighth largest world producer, behind the US, China, Italy, Spain, Turkey, Portugal and Iran (WPTC, 2016). In this scenario, the concern with the mineral nutrition of the plant, which can

represent gain or loss in productivity, is common among farmers and accurate soil fertilization is constant discussion in the scientific community.

Knowledge of the accumulation of nutrients by the culture throughout the life cycle can help in decision making about the best time to split fertilization. Researches on biomass and nutrients accumulation curves from tomato, especially cultivars for industry, are scarce. What is found in the literature are classic works as Gargantini and White (1963) and Haag et al. (1978), both carried out with old cultivars and in different environmental conditions of current conditions. Other existing work, but with cultivars for fresh consuming, have demonstrated varying amounts of biomass and tomato nutrient uptake, due different conditions of management and environments (Scholberg et al, 2000a;. Fayad et al., 2002; Prado et al ., 2011; Lucena et al, 2013).

This research was accomplished in order to characterize the curves of accumulation of biomass and nutrients of processing tomato grown in soils with different levels of fertility.

Material and Methods

Two experiments were carried out in the period from May 15 to Sept. 2 of 2013, in rural properties in Guaíra city, state of São Paulo-Brazil (20º27'S lat; 48º19'W long). The climatic classification is tropical with dry winter (Köppen = Aw; Thornthwaite = B_1rA'a'), and the annual average rainfall is 1374 mm.

The soil at the experimental sites is classified as Typic Hapludox (highly weathered deep clay soil), with 52% clay, 29% silt, and 19% sand, but different chemical characteristics. The experiment 1 was conducted in soil with pH$_{(CaCl_2)}$ 5.6; organic matter (OM) = 29 g dm^{-3}; P = 116 mg dm^{-3}; K = 3.5; Ca = 28; Mg = 6; H + Al = 29; cation exchange capacity (CEC) = 66 mmol$_c$ dm^{-3}, and bases saturation (V) = 57 % (percentage of CEC filled by K, Ca, and Mg), which was considered high fertility (HF). The soil of experiment 2 had pH $_{(CaCl_2)}$ 4.5;

OM = 26 g dm^{-3}; P = 8 mg dm^{-3}; K = 1.1; Ca = 8; Mg = 6; H + Al = 36; CEC = 51 $mmol_c$ dm^{-3}; V = 30 %, which was considered low fertility (LF).

Two months before transplanting the areas were plowed and received liming to raise V to 80%. At transplant rows were opened where it was held the application of 30 kg ha^{-1} N (urea), 160 kg ha^{-1} of K_2O (potassium chloride) and 450 kg ha^{-1} P_2O_5 (superphosphate triple). This fertilization is commonly used by farmers regardless of soil fertility. Then the rows were closed and it was realized mechanical transplanting of tomato 'Heinz-9553' in spacing 1.25 m x 0.25 m. For top-dressing 60 kg ha^{-1} N (urea) at 30 days after transplanting (DAT), and the amount of 160 kg ha^{-1} K_2O was divided in three applications at 45, 65 and 85 DAT were applied. The crop was weekly irrigated by center pivot with application of 25 mm of water from transplanting to early flowering and 40 mm from flowering to five days before harvest, always discounting rainfall during the period.

The beginning of flowering occurred at 40 DAT when it were collected leaf samples to assess the nutritional status of tomato plants, according to recommendation of Fontes (2000).

To estimate the accumulation curves of biomass and nutrient absorption by processing tomato ten plants collection times (30, 40, 50, 60, 70, 80, 90, 100, 110, 120 DAT) in four replications (three plants per replication) was adopted. In each collection, the plants were divided into vegetative parts (leaves + stems) and reproductive (fruit).

For assess the nutritional status and to estimate the accumulation of nutrients in the parts of the plant, the material was washed in running water, detergent solution (1 ml L^{-1}), then rinsed in deionized water three times. The washed material was placed to dry in an oven with forced air circulation at 65 °C until constant mass. The dried samples were ground in a Willey mill using a 0.1 mm mesh sieve. The analysis to determine nutrients content on plants were performed according to methods of Tedesco et al. (1995).

It were determined macronutrients and micronutrients accumulated in vegetative tissue and in fruits tissue at each collect date. The accumulation (Ac) of nutrients in each part of plant and in each sampled date was obtained by: Ac = Nc * DM, where: Nc= nutrient concentration and DM= dry mass of the part that was obtained Nc, at the time of sampling.

The data of biomass and nutrient accumulation in processing tomato grown on soils with HF and LF were submitted to polynomial regression analysis for construction of accumulation curves during crop life cycle (Table 1).

Table 1: Number of days after transplant to change phenological phases**.**

Phenological phase	Days after transplant
Starting flowering	40
Fruiting initiation	55
Starting fruit color changing (green to red)	85
50% of fruits red	105
80% of fruits red	120

Results and Discussion

The accumulation of biomass in vegetative parts (leaves+stem) (VB) and fruits biomass (FB) of tomato grown in soils with high fertility (HF) and low fertility (LF), was described by a quadratic model (Figure 1). Although with the same polynomial adjust, the accumulation of VB of tomato plants showed different patterns of intensity of accumulation in HF and LF while FB accumulations were very similar in both soils.

The maximum accumulation of VB of tomato plants grown in soil with HF (105.5 g plant^{-1}) and in LF (72.2 g plant^{-1}) were achieved at 83 and 87 DAT, respectively. For the period post-transplant to maximum VB, the rates of VB accumulation were 1.3 and 0.8 g plant^{-1} day^{-1}, respectively in HF and LF. However, for the period from the beginning of flowering (40 DAT) to the maximum accumulation of VB, the accumulation rates were 1.5 and 0.9 g plant^{-1} day^{-1} in tomato plants grown in soil with HF and LF, respectively. Therefore,

two points can be highlighted: first the VB increment rate of tomato plants grown in soils with HF is higher than tomato plants grown in soil with LF in both periods evaluated, and second the VB accumulation is higher after the beginning of flowering than earlier.

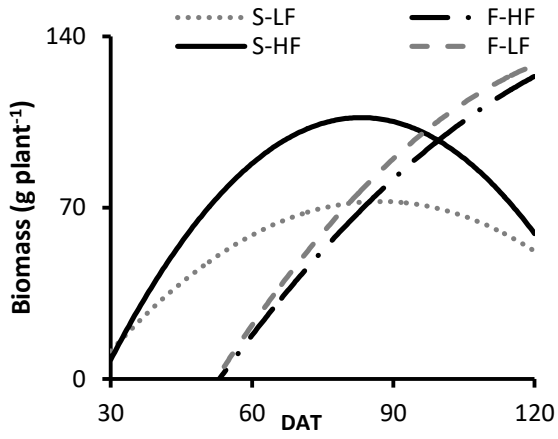

Figure 1: Biomass accumulation of processing tomato grown in high and low fertility soils. VB = vegetative biomass, F = fruit biomass, HF = High Fertility, LF = Low Fertility.

After 83 (HF) and 87 (LF) DAT, it were observed reductions in amounts of accumulated VB of tomato plants, reaching similar amounts at harvest in both fertility conditions. This fact can be explained by senescence of older leaves (Scholberg et al. 2000a) due to redistribution of nutrients, especially N, to fruits (Boote et al., 2006). Scholberg et al. (2000a) also observed deceleration in VB accumulation of fresh tomato from 42 DAT, when it began the rapid growth of fruits.

The FB accumulation of plants grown in HF and LF exceeded VB accumulation at 99 and 82 DAT, respectively (Figure 1). At harvest FB was equivalent to 68% and 71% of the total biomass accumulated in plants grown in soil with HF and LF, respectively. Therefore, it is noted that although the higher amount of VB accumulated plants grown in HF soil were higher than those plants grown in LF soil, the amounts of biomass allocated in fruits of plants

grown in both soils were close, with slightly higher value observed for plants grown in soil with LF (128 g plant^{-1}) than in HF (124 g plant^{-1}). It is possible to infer that plants grown in HF soil and fertilized the way they were, had excessive growth of the vegetative parts, not converting the "high productive potential" (due to higher possibility to make photosynthesis) in increased production of FB. It can happen due to the auto shading of the plants, which reduces the use of radiation and the photosynthetic rate of the plants, thus reducing the distribution of photoassimilates for fruit filling (Wamser et al., 2007).

The accumulation of nutrients followed the growth of plants and the uptake of all nutrients was intensified at beginning of flowering. Nitrogen accumulation in VB and the total accumulated in whole plants of tomato 'Heinz 9553' occurred quadratically in HF and LF, while fruits (FB) had linear increase of N (Figure 2A).

Until the beginning of flowering (40 DAT), tomato plants grown in soil HF and LF had accumulated 51% and 60% of the maximum N accumulated in VB, respectively. The maximum accumulation of N in VB reached 2.7 g plant^{-1} at 78 DAT in HF soil, and 1.7 g plant^{-1} at 77 DAT in LF soil, equivalent to 66% (in HF) and 35% (in LF) of the total accumulated by the plant at harvest.

Fruits accumulate N linearly. The reduction of N accumulated in tomato VB can be explained by the redistribution of N from leaves to fruits and by the senescence and leaf abscission that occurs during the fruiting period, and more intensely with the proximity of fruit maturation.

At harvest, the fruits presented 83% and 82% of N total accumulated by plants in HF and LF soils, respectively. Scholberg et al. (2000b) observed that at the beginning of fruiting, the accumulation in the VB of tomato corresponded to 60% of total N accumulated and decreased to 39% at harvest, because of the increased accumulation in fruits. The total N

accumulated at 120 DAT were 4.41g plant^{-1} in HF soil and 4.72 g plant^{-1} in LF soil, therefore similar.

Plants grown in LF had quadratic adjustment for K accumulation in VB and linear adjustment for K accumulation in FB and in whole plants, while plants grown in HF accumulated K with quadratic adjustment in VB and FB and cubic adjustment for the whole plant (Figure 2B). The maximum accumulation of K in VB was 4.6 g plant^{-1} at 76 DAT in HF and 2.4 g plant^{-1} at 82 DAT in LF.

At the beginning of flowering (40 DAP), K accumulated in VB of plants were 27% and 15% in plants grown in HF and LF soil, respectively, of the total K accumulated in whole plants at end of season. At beginning of fruiting it was observed increase in daily accumulation rate of K (kg ha^{-1} day^{-1}) by tomato plants of 0.8 (40 DAT) to 1.5 (50 DAT) and then to 2.1 (60 DAT) in LF and of 1.4 (40 DAT) to 2.2 (50 DAT) and then to 3.0 (60 DAT) in HF.

The increase in K accumulation rate at the beginning of the reproductive phase occurs because of high demand for nutrients by fruits. The high mobility of K causes it to be easily redistributed in the plant with the appearance of new drains (Hawkesford et al., 2012). In tomato plants the fruits are the main drains and, at the beginning of reproductive phase, start to accumulate more K (Scholberg et al, 2000a;. Fayad et al., 2002; Boote et al., 2006). Deceleration was observed in the accumulation of K by VB due to the high demand for K by the fruit. At harvest, plants in HF accumulated the total of 4.5 g plant^{-1} of K, 2.7 g plant^{-1} in FR and plants in LF accumulated the total of 8.5 g plant^{-1} of K and 6.5 g plant^{-1} in FR.

The increase on demand for N and K by processing tomato occurred at beginning of flowering (40 DAT) (Figure 3). This result indicates that the application of N and K as

covering fertilization at flowering to early fruiting can benefit plants and increase productivity.

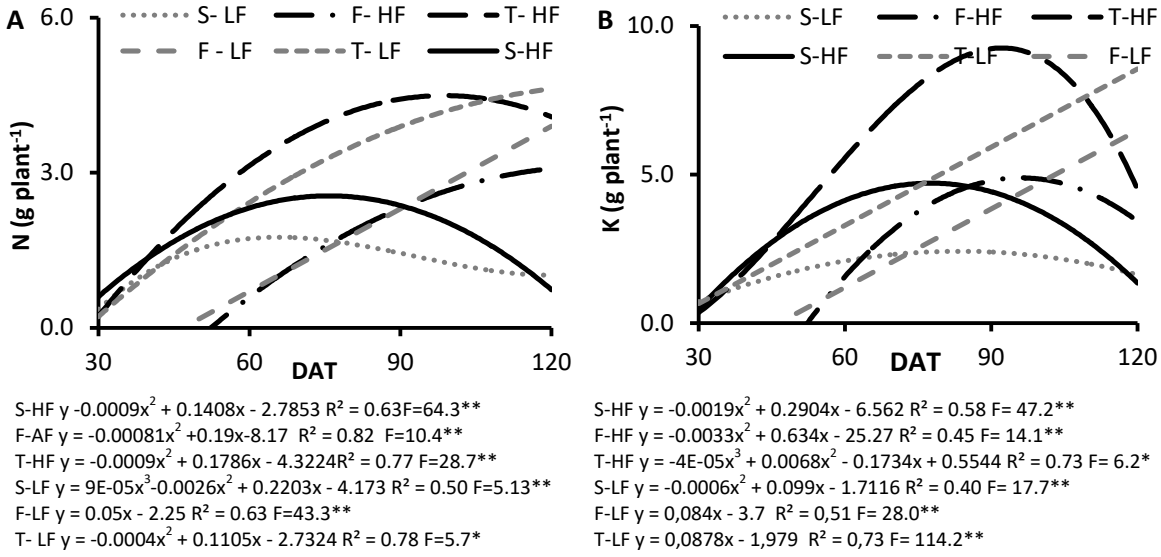

Figure 2: Nitrogen (A) and Potassium (B) accumulation in processing tomatoes grown in high and low fertility soils. S=Shoot, F= Fruit, T=Total (fruit + shoot), HF = High Fertility, LF = Low Fertility.

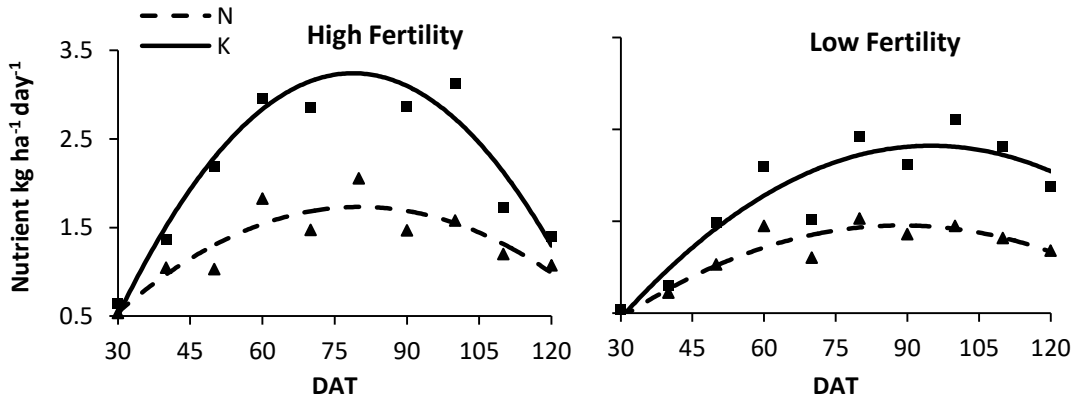

Figure 3: Daily accumulation of N and K in processing tomato grown in high and low fertility soil.

The accumulation of P had cubic adjustment in VB and quadratic adjustment in FR and in the whole plant, when grown in HF; and cubic adjustment in VB, linear in FR, and quadratic in the whole plants when grown in LF. Plants in HF reached the maximum accumulation of 1.03 g plant^{-1}of P at 100 DAT and 0.95 g plant^{-1}of P at harvest (120 DAT). In

LF maximum accumulation of P was 0.90 g plant^{-1} and occurred at harvest time (120 DAT) (Figure 4A), therefore the total amount of accumulated P in plants in HF and LF was similar.

As well for N and K, deceleration was observed in the accumulation of P in VB due to increased demand of this nutrient by fruits. At harvest, fruits accumulated 0.89 and 0.77 g plant^{-1} P, equivalent to 94% and 86% of total P accumulated in plants grown in HF and LF soils, respectively. Plants in general accumulate large amount of P in fruits because this nutrient is stored in the seeds as phytate, which is one source of P during the germination process (Hawkesford et al., 2012).

The plants in HF presented quadratic adjustment for Ca accumulation in VB, FR and whole plant. In LF, the plants accumulated Ca with quadratic adjustment in VB and in whole plant and linear adjustment in FR (Fig. 4B). The maximum amount of accumulated Ca in VB was 3.4 and 2.5 g plant^{-1} at 84 and 91 DAT in HF and LF, respectively. In FR Ca accumulation was very low compared to the accumulation in the VB, reaching 0.20 and 0.26 g plant^{-1} equivalent to 10% and 12% of the total Ca accumulated in plants at 120 DAT in HF and LF, respectively.

The highest accumulation of Ca on VB is because this nutrient is mainly transported by the xylem in favor of the transpiration stream, and has low redistribution in the plant. This is because most of Ca contained in plants is calcium pectate, a component of middle lamella of the cell wall, as well as low-solubility salts such as carbonate, sulfate, phosphate, etc. Due to low solubility and low concentration of Ca in the phloem, redistribution it is very limited and therefore the fruits tend to receive less Ca (Hawkesford et al, 2012;. Malavolta et al., 1997).

During the tomato plants cycle, the amounts of Ca accumulated by plants were different in soils with HF and LF; however, at the end of the cycle (120 DAT) the total of Ca

accumulated per plant was very similar in both fertility conditions, equivalent to 2.0 g plant^{-1} HF, and 2.2 g plant^{-1} in LF.

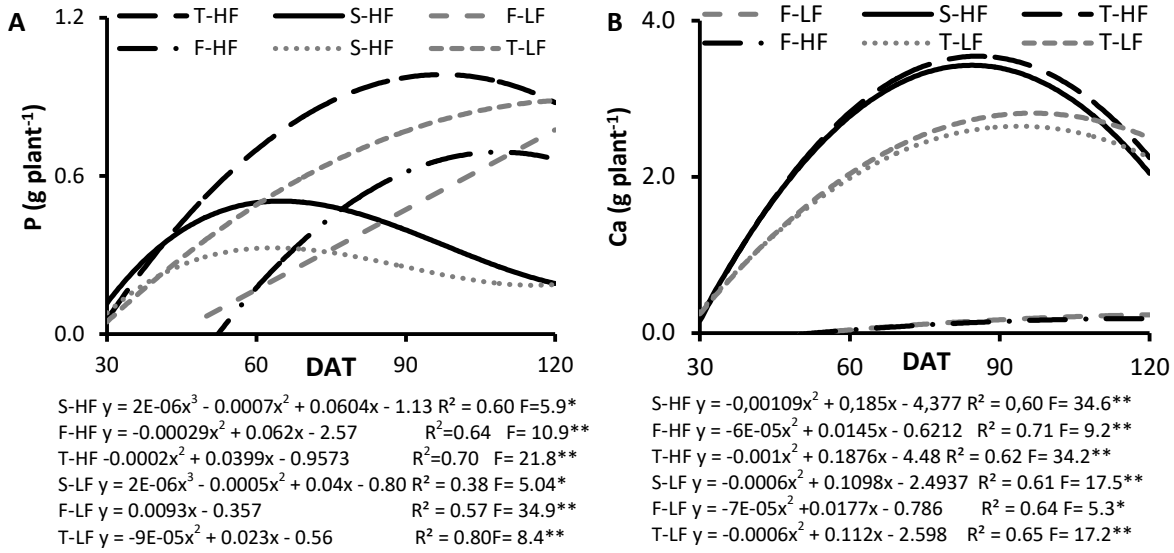

Figure 4: Phosphorus (A) and Calcium (B) accumulation in processing tomato grown in high and low fertility soils. S=Shoot, F= Fruit, T=Total (fruit + shoot), HF = High Fertility, LF = Low Fertility.

Magnesium was accumulated with quadratic adjustment in VB, FR and total in whole plants grown in HF and LF. As observed for Ca, Mg was preferentially accumulated in the vegetative organs of the plant (Figure 5A), but in smaller quantities. The maximum amount of accumulated Mg in VB was 0.77 g plant^{-1} at 90 DAT in HF and 0.70 g plant^{-1} at 85 DAT in LF. At harvest (120 DAT), the amounts of Mg accumulated in whole plants were 0.65 g plant $^{-1}$ in HF and 0.85 g plant^{-1} in LF. It was observed deceleration in the Mg accumulation by plants with the proximity of the harvest (fruit maturity) that may be associated with senescence of older leaves.

The main function of Mg is to be part of the chlorophyll molecules in green leaves. The total quantity of Mg in chlorophyll molecules depends on the availability of this nutrient to the plant. Plants well nourished of Mg can accumulate up to 25% of Mg in the leaves,

therefore senescence of leaves is important mechanism of loss of accumulated Mg in plants (Hawkesford et al., 2012).

The amount of Mg accumulated in FR at harvest in both soils was 0.28 g plant^{-1}, equivalent to 34% and 44% of the total Mg accumulated in the whole plant grown in LF and HF, respectively. In general, tomato fruits have smaller accumulation of Mg than VB, similar result was also observed by Fayad et al. (2002), Prado et al. (2011) and Lucena et al. (2013) for fresh tomato grown on field, greenhouse and hydroponics.

The accumulation of Sulfur had quadratic adjustment in VB, FR and total (whole plants) grown in HF and LF (Figure 5B). The maximum accumulation of S in PV was 0.42 g plant^{-1} at 76 DAT in HF and 0.37 g plant^{-1} at 88 DAT in LF. The FR of plants grown in HF and LF also showed S accumulation similar throughout the cycle, with maximum of 0.25 g plant^{-1} in HF and 0.19 g plant^{-1} in LF at 120 DAT. Despite the difference in the S accumulation in the VB, plants in HF and LF during the crop cycle, at harvest the total of S accumulated in whole plants was 0.67 g plant^{-1} in LF and 0.53 g plant^{-1} in HF, therefore similar.

It was observed a slight decrease in the amount of S accumulated in the VB due to redistribution of nutrient for fruits. At harvest, the fruits contained 48% and 28% of the total S uptake by plants grown in HF and LF, respectively. Different result was obtained by Fayad et al. (2002), where fruits of fresh tomatoes, grown in field and greenhouse, accumulated 20% and 23%, respectively, of total S accumulated at harvest.

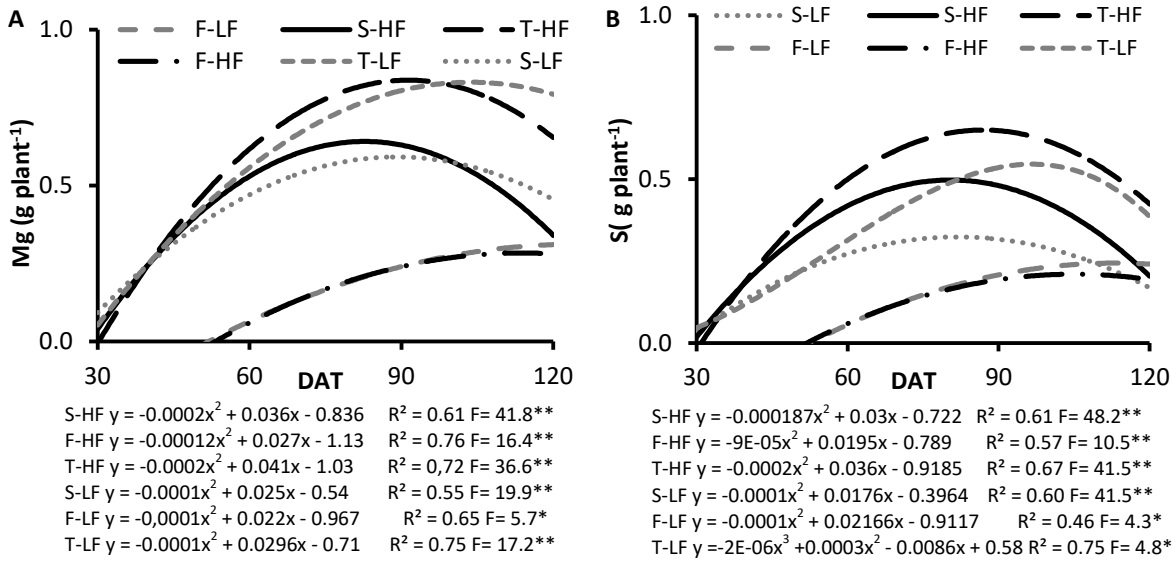

Figure 5: Magnesium (A) and Sulfur (B) accumulation in processing tomato grown in high and low fertility soils. S=Shoot, F= Fruit, T=Total (fruit + shoot), HF = High Fertility, LF = Low Fertility.

The nutrients N, K and P were accumulated preferably in FR, while the highest amount of Mg, Ca and S was accumulated in VB of plants, with the exception of S in LF that was accumulated in highest quantity in VB. The same distribution of nutrients in tomato plants was observed by Fayad et al. (2002), Prado et al. (2011) and Lucena et al. (2013) in fresh tomato cultivars in various environmental conditions. The total amounts of macronutrients and biomass accumulated per hectare at 120 DAT in HF and LF are shown in Table 2.

Table 2: Nutrients (kg ha^{-1}) and Biomass (t ha^{-1}) accumulation in processing tomato grown in high and low fertility soils. Total (fruit + leaves + stems) and in fruits at 120 DAT.

Nutrients	N	P	K	Ca	Mg	S	Biomass
			High Fertility				
Total	129	29	168	71	19.5	13	6.0
Fruits	100	23	126	6	9	6	4.0
			Low Fertility				
Total	142	26	226	71	22.5	12	5.6
Fruits	113	23	177	7	9	6	4.0

The nutrients Fe, Cu, Mn and Zn were preferably accumulated in the VB of plants (Figure 6) and the redistribution to FR was small. This result is similar to those obtained by Fayad et al. (2002) and Rodrigues et al. (2002), who also found highest accumulation of these nutrients in the VB of fresh tomato.

Iron was the micronutrient accumulated in highest amounts in HF and LF, with cubic adjustment in VB and quadratic adjustment in FR and total in whole plants in HF. Plants grown in LF accumulated Fe with quadratic adjustment in VB and FR and cubic adjustment for total in whole plants. Fe accumulation was higher in plants in LF with a total accumulation of 73.4 mg plant^{-1} at 120 DAT, while plants in HF accumulated 31.6 mg plant^{-1} at the same date. The high requirement of Fe for maintaining structural and functional integrity of the thylakoids and the additional demand Fe for ferredoxin and chlorophyll biosynthesis explain the high amount of Fe accumulated mainly in the leaves (Broadley et al., 2012).

Copper was accumulated with quadratic adjustment in FR and total (whole plants) and cubic adjustment in VB in plants grown in HF soil. Plants in LF soil accumulated Cu with linear adjustment in FR, cubic in VB, and quadratic for total accumulation. The fruits accumulated low amount of Cu compared to VB in both fertility levels. Cupper accumulated in whole plants at 120 DAT was 26.5 mg plant^{-1} HF and 24.2 mg plant^{-1} in LF, while fruits accumulated 1.8 mg plant^{-1} in HF and 2.3 mg plant^{-1} in LF. High accumulation of Cu in VB occurs because this micronutrient is part of enzymes present in the chloroplast and participates in photosynthesis process (Silva et al, 2012).

Manganese accumulation was similar to Cu accumulation in LF with cubic adjustment in PV and total (whole plant) and linear in FR. In HF, the adjustment was quadratic in PV, FR and total. Mn participates in chlorophyll synthesis and plays important roles in

photosynthesis, therefore, the highest accumulation occurs in leaves and a small amount is redistributed to the fruit (Silva et al., 2012). In FR, the maximum of Mn accumulated was 2.8 mg plant^{-1} HF and 3.2 mg plant^{-1} in LF at harvest (120 DAT), equivalent to 30% and 18% of the total accumulated in whole plants at 120 DAT, respectively.

Among the micronutrients, Zn was the less accumulated in processing tomato. Similar result was obtained by Fayad et al. (2002) for fresh tomato, however, Rodrigues et al. (2002) obtained Zn as the third most accumulated micronutrient in tomato plants. Plants in HF accumulated Zn with quadratic adjustment in VB, FR and total. The plants grown in LF accumulated Zn with linear adjustment in VB and FR and cubic adjustment in total. The maximum accumulation of Zn in VB of plants grown in HF was 16.1 mg plant^{-1} at 85 DAT, higher value than the observed in plants grown in LF which was 9.3 mg^{-1} plant at harvest. Although the differences in Zn accumulation in VB, in FR the accumulation was similar in both soils, with accumulation of 13 mg plant^{-1} in HF and 19 mg plant^{-1} in LF at 120 DAT.

At harvest, the total accumulated of Fe, Cu, Mn and Zn decreased, contrary of linear accumulations of micronutrients in fresh tomatoes obtained by Fayad et al. (2002). The decreases in the amounts of micronutrients accumulated close to the end of plant cycle, probably occur due to reduction of VB, since these micronutrients were accumulated in higher amounts in leaves and stems.

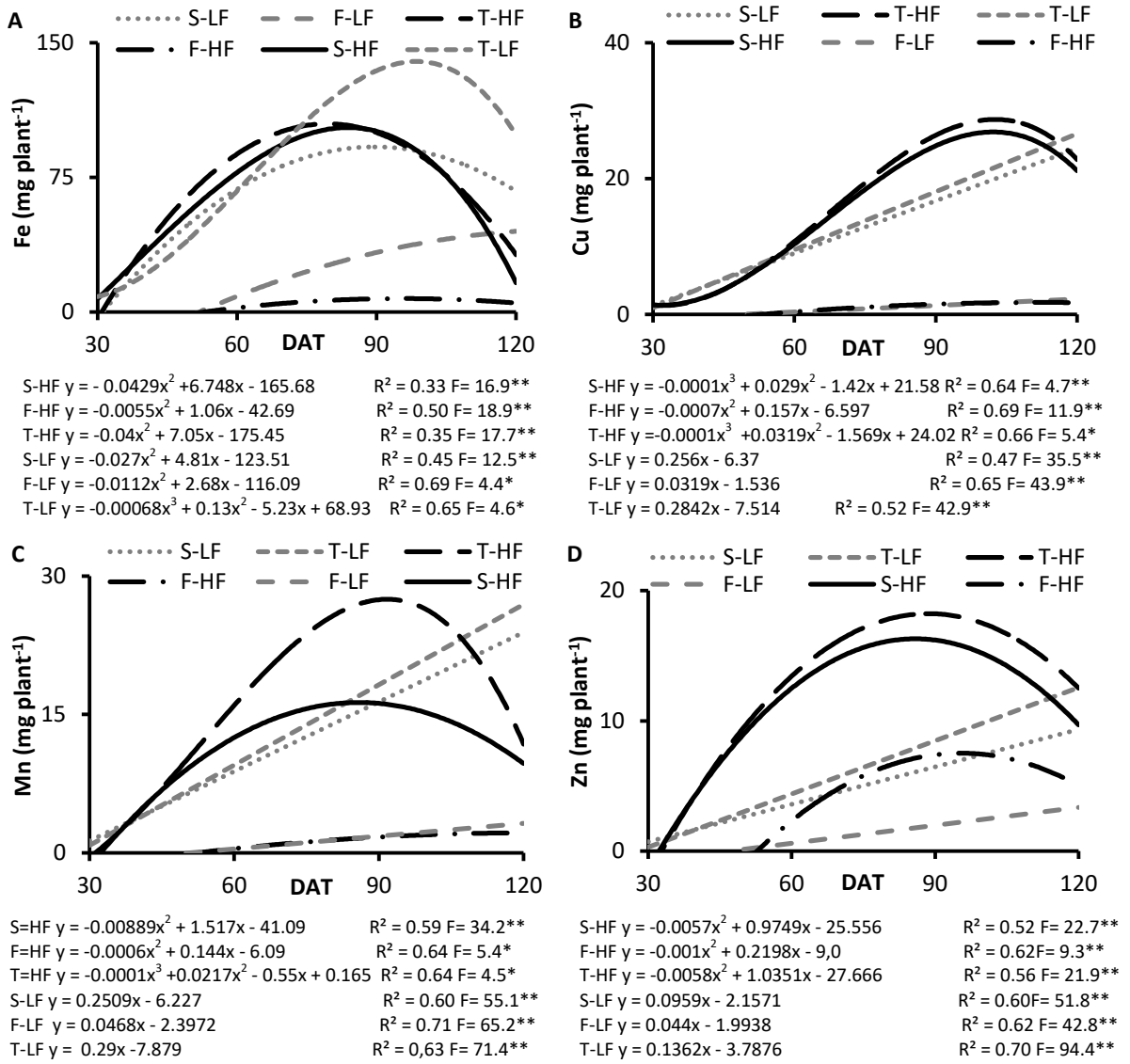

Figure 6: Iron (A), Cupper (B), Manganese (C), and Zinc (D) accumulation in processing tomato grown in high and low fertility soils. S=Shoot, F= Fruit, T=Total (fruit + shoot), HF = High Fertility, LF = Low Fertility.

At harvest (120 DAT), the fruits in LF had accumulated 55% Fe, 13% Cu, 17% Mn and 33% Zn of the total accumulated in the whole plant. In HF, the fruits had accumulated 22% Fe, 7% Cu, 19% Mn and 22% Zn of the total cumulated in the whole plant. The total accumulation of Fe, Cu, Mn and Zn was 27.3, 24.1, 12.8 and 11.8 mg plant^{-1}, respectively, in HF; and 77.8, 15.4, 17.5 and 8.8 mg plant-1, respectively, in LF. The amounts of

micronutrient accumulated in fruits and in whole plants per hectare at 120 DAT, in HF and LF are shown in Table 3.

Table 3: Micronutrients (g ha^{-1}) accumulation in processing tomato grown in high and low fertility soils. Total (fruit + leaves + stem) and in fruits at 120 DAT.

Nutrient	Cu	Fe	Mn	Zn
		High Fertility		
Total	777	881	413	381
Fruits	58	190	77	84
		Low Fertility		
Total	497	2510	565	284
Fruits	68	1377	94	94

Potassium was the most accumulated nutrient in processing tomato in both soils, HF and LF, followed by N, Ca, P, Mg and S. Lucena et al. (2013) obtained K, N, Ca, Mg and P as descending order of macronutrient accumulation in tomato cultivar 'MS-16' grown on field. For the cultivar Santa Clara, also grown on field, Fayad et al. (2002) obtained K, N, Ca, S, P and Mg as descending order and for the hybrid EF-50 cultivated in greenhouse K, N, Ca, S, Mg and P. These results indicate that K it is the most accumulated nutrient by tomato, independent of cultivar or cropping system.

For micronutrients, it was observed the following descending order of accumulation: Fe, Cu, Mn, Zn in plants grown in HF, and Fe, Mn, Cu, Zn in plants grown in LF. Fayad et al. (2002) observed the descending order of accumulation of micronutrients for fresh tomato Cu, Mn, Fe and Zn, when grown on field, and Mn, Fe, Cu and Zn when grown in greenhouse.

Table 4: Nutrient contents in processing tomato grown in low fertility (LF) and high fertility (HF) soils, and nutrient contents recommended by Silva and Giordano (2000).

Fertility levels	N	P	K	Ca	Mg	S	Cu	Fe	Mn	Zn
	----------g/kg----------						----------mg/kg----------			
LF	35	7	37	34	9	5	81	688	95	52
HF	38	9	50	29	6	5	67	1028	99	65
Silva and Giordano (2000)	40-60	2.5-7.5	30-50	15-30	4-6	4-12	10-20	400-600	250-400	60-70

Leaf contents for the assessment of nutritional status of tomato plants grown in soil with HF and LF are shown in Table 4, as well as the levels considered adequate by Silva and Giordano (2000). The levels indicate contents of N and Mn below the adequate in HF and LF, and also for Zn content in LF. Although detected these deficiencies, plants in HF had productivity of 142 t ha^{-1} and 122 t ha^{-1} in LF, considered high.

Conclusion

Processing tomato grown in soil with high fertility level can accumulate more nutrients in vegetative organs than plants in soil with low fertility level, however the higher accumulation of nutrients is not converted in higher production of biomass per plant.

The accumulation of biomass and nutrients increases after the beginning of flowering until the fruit color changes, so this is the period of the highest demand for nutrients, especially N and K, when the farmer should pay attention to provide adequate fertilization.

Plants of processing tomato grown in high and low fertility soils those received same crop management, including fertilization, have similar potential of biomass production per plants but different productivity.

References

BOOTE, K. J.; RYBAK, M. R.; SCHOLBERG,J. M. S.; JONES, J. W. Improving the CROPGRO-Tomato Model for Predicting Growth and Yield Response to Temperature. HortScience. v. 47, p 1038-1049, 2012.

BROADLEY, M.; BROWN, P.; CAKMAK, I.; RENGEL, Z.; ZHAO, F. Functions of Nutrients: micronutrients. In: MARSCHNER P. 2012. Mineral nutrition of higher plants. San Diego: Elsevier, 651p.

ENGELS, C.; KIRKBY, E.; WHITE, P. Mineral Nutrition, Yield and Source-Sink Relationships. In: MARSCHNER P. 2012. Mineral nutrition of higher plants. San Diego: Elsevier, 651p.

FAYAD, J. A.; FONTES, P. C. R.; CARDOSO, A. A.; FINGER, F. L.; FERREIRA, F. A. Absorção de nutrientes pelo tomateiro cultivado sob condições de campo e de ambiente protegido. Horticultura brasileira. v. 20, p. 90-94, 2002.

FONTES, R. R. Solo e nutrição da planta. In: SILVA, J. B. C.; GIORDANO, L. B. Tomate para processamento industrial, 1 ed. Brasilia: Embrapa, 2000.

GARGANTINI, H.; BLANCO, H. G. Marcha de absorção de nutrientes pelo tomateiro. Bragantia, Piracicaba,v. 22, n. 1, p. 693-714,1963.

HAAG, H. P.; OLIVEIRA, G. D.; BARBOSA, V.; SILVA NETO, J. M. Marcha de absorção de nutrientes pelo tomateiro (*Lycopersicon esculentum* Mill), destinado ao processamento industrial. Anais da Escola Superior de Agricultura “Luiz de Queiroz”, Piracicaba,v. 35, n. 2, p. 243-269,1978.

HAWKESFORD, M.; HORST, W.; KICHEY, T.; LAMBERS, H.; SCHJOERRING, J.; MOLLER, I. S.; WHITE, P. Functions of Macronutrients. In: MARSCHNER P. 2012. Mineral nutrition of higher plants. San Diego: Elsevier, 651p.

LUCENA RRM; NEGREIROS MZ; MEDEIROS JF; BATISTA TMV; BESSA ATM; LOPES WAR. Acúmulo de massa seca e nutrientes pelo tomateiro 'SM-16' cultivado em solo com diferentes coberturas. Horticultura Brasileira. v 31, p. 401-409. 2013

MALAVOLTA, E.; VITTI, G.C.; OLIVEIRA, S.A. 1997. Avaliação do estado nutricional das plantas. Piracicaba: Potafos, 204p.

PRADO, R. M.; SANTOS, V. H. G.; GONDIM, A. R. O.; ALVES, A. U.; CECÍLIO FILHO, A. B.; CORREIA, M. A. R. Crescimento e marcha de absorção de nutrientes em tomateiro cultivar Raísa cultivado em sistema hidropônico. Semina: Ciências Agrárias. v 32, p. 19-30. 2011

RODRIGUES, S. D.; PONTES, A. L.; MINAMI, K.; DIAS, C. T. S. Quantidade absorvida e concentrações de micronutrientes em tomateiro sob cultivo protegido. Scientia Agricola, Piracicaba, v. 59, n. 1, p. 137-141, 2002.

SCHOBERG, J.; MCNEAL, B. L.; JONES, J. W.; BOOTE, K. J.; STANLEY, C. D.; OBREZA, T. A. Growth and Canopy Characteristics of Field-Grown Tomato. Agronomy Journal. v 92. p.152-159. 2000a.

SCHOBERG, J.; MCNEAL, B. L.; BOOTE, K. J.; JONES, J. W.; LOCASCIO, SAL J.; OLSON, S. M. Nitrogen Stress Effects on Growth and Nitrogen Accumulation by Field-Growth Tomato. Agronomy Journal. v 92. p.159-167. 2000b.

SILVA, J.; GUEDES, I. M. R.; LIMA, C. E. P.Adubação e nutrição. In: CLEMENTE, F. M. V.T.; BOITEUX, L. S. Produção de Tomate para Processamento Industrial. Brasília: EMBRAPA, 2012. p. 105-127.

TEDESCO, M. J.; GIANELLO, C.; BISSANI, C. A.; BOHNEN, H.; VOLKWEISS, S. J. Análise de solo, plantas e outros materiais. Porto Alegre, Universidade Federal do Rio Grande do Sul, 1995. 174p. *Boletim técnico, 5*.

TRANI, P. E.; NAGAI, H.; PASSOS, F. A.Tomate rasteiro (industrial) irrigado. In: RAIJ, B. van; CANTARELLA, H.; QUAGGIO, J. A.; FURLANI, A.M.C. Boletim Técnico n.100 - Recomendações de adubação e calagem para o Estado de São Paulo. 2.ed. Campinas: IAC, 1997. p.184-185.

WAMSER, A. F; MUELLER, S; BECKER, W. F; SANTOS, J. P. Fruits production of tomatoes as a result of plant training systems. Horticultura Brasileira, v. 25, n. 2, p. 238-243, 2007.

WPTC- World Processing Tomato Council. Releases. Disponível em: <http://www.wptc.to/releases-wptc.php>. Acesso em: 19/01. 2016.